SMARTSAT
COOPERATIVE RESEARCH CENTRE

TECHNICAL REPORT AQW-4

AquaWatch Pilot Project: Aquaculture in Spencer Gulf

TECHNICAL REPORT AQW-4

AquaWatch Pilot Project: Aquaculture in Spencer Gulf

JUNE 2023

SMARTSAT COOPERATIVE RESEARCH CENTRE

CSIRO

Copyright © SmartSat CRC Ltd, 2023

This book is copyright. Except as permitted under the Australian Copyright Act 1968 (Commonwealth) and subsequent amendments, no part of this publication may be reproduced, stored or transmitted in any form or by any means, electronic or otherwise, without the specific written permission of the copyright owner.

This report should be cited as:
SmartSat 2023, AquaWatch Pilot Project: Aquaculture in Spencer Gulf, SmartSat Technical Report AQW-4, SmartSat, Adelaide, Australia.

Disclaimer:
This publication is provided for the purpose of disseminating information relating to scientific and technical matters. Participating organisations of SmartSat do not accept liability for any loss and/or damage, including financial loss, resulting from the reliance upon any information, advice or recommendations contained in this publication. The contents of this publication should not necessarily be taken to represent the views of the participating organisations.

Acknowledgement:
SmartSat acknowledges the contribution made by AquaWatch Australia team, AquaWatch Data Integration and Analytics System (ADIAS, powered by EASI) team and South Australian Research and Development Institute (SARDI) team towards writing and compilation of this technical report.

Project (P3-17) team would also like to acknowledge, SARDI field and technical team (Ian Moody and crew of the RV Ngerin), University of Adelaide team (Nguyen Thanh Toan Le and Ken Clarke), CSIRO Bio-Optics Lab (Bozena Wojtasiewicz and Elizabeth Brewer), CSIRO Aquatic Remote Sensing Team (Gemma Kerrisk), HydraSpectra team (Tim Malthus, Erin Kenna and Faisal Islam) for their technical support for this project.

Executive Summary

The AquaWatch pilot project (P3-17) aims to establish an effective water quality monitoring system in the Boston Bay region of Spencer Gulf, an area which encompasses one of the most diverse and productive aquaculture sectors in South Australia. The project design emphasizes the importance of integrating multiple data streams from *in situ* and satellite platforms to enhance the accuracy and reliability of water quality assessments.

The project successfully implemented a comprehensive sensor selection, buoy design, and installation plan. The site selection process involved collaboration with project partners at the South Australian Research and Development Institute (SARDI) to identify a suitable location that met essential requirements such as water depth, surface stability and proximity to aquaculture activities.

A monitoring station, consisting of a buoy platform integrated with a range of instruments and devices, was deployed to ensure precise measurements and calibration/validation of earth observation data. The selection of sensors included both above and below-water options such as the HydraSpectra sensor, Xylem YSI multiparameter sonde, and a harmful algal index (HAI) sensor for on-site measurements. The Xylem DB1750 buoy was specifically chosen for its stability in the sea conditions of the region. Power was provided through solar panels and a rechargeable battery, while data logging and telemetry modules facilitated wireless transmission of sensor data. The deployed system encompasses various components, including the HydraSpectra sensor for above-water surface reflectance measurements, an Xylem YSI multiparameter sonde and harmful algal index (HAI) sensor for in-water measurements, a weather station, GPS, and sea light. The live data streams from the HydraSpectra sensor are transmitted to the CSIRO Senaps IoT platform for processing, while data from other sensors are uploaded and visualized using the Eagle.io platform.

The AquaWatch Data Integration and Analysis System (ADIAS) platform serves as a cloud-based data warehouse and analysis platform for the AquaWatch project. It facilitates the ingestion, tracking, processing, and analysis of *in situ* and remote sensing data. The in-situ data pipeline consolidates data from various sensors in a purpose-built datalake, enabling easy access and analysis through a single SQL interface in the ADIAS platform.

Empirical algorithm development and evaluation were conducted to derive water quality information from the integrated *in situ* and remote sensing data. The algorithm development process involved calibrating and quality-assuring the in-water and radiometric data, convolving the radiometric data to match the spectral resolution of the intended remote sensing sensor, and establishing empirical relationships between spectral features and water quality parameters.

Overall, the AquaWatch project has successfully implemented a comprehensive water quality monitoring system that integrates *in situ* and satellite observations. The project's design, sensor selection, buoy installation, and data integration efforts have resulted in a cohesive data delivery system that provides timely and reliable water quality data for informed decision-making and effective management of the coastal aquaculture ecosystem in the Boston Bay region of Spencer Gulf. Several recommendations on in situ sensing, remote sensing, and their integration in AquaWatch analytics platform were also presented.

Acronyms and notation

ADIAS – AquaWatch Dara Integration and Analytical System

AOP – Apparent Optical Properties

CDOM—Coloured Dissolved Organic Matter

CSIRO – Commonwealth Scientific and Industrial Research Organisation

DO – Dissolved Oxygen

DOC – Dissolved Organic Matter

fDOM – Fluorescent Dissolved Organic Matter

fCHL - Fluorescence from Chlorophyll.

HAB – Harmful Algal Blooms

HAI – Harmful Algal Index

HPLC – High-performance liquid chromatography

IOP – Inherent Optical properties

NASA - The National Aeronautics and Space Administration

NTU - Nephelometric Turbidity Units

SARDI – South Australian Research and Development Institute

SIOP – Specific Inherent Optical Properties

TSS – Total Suspended Sediment

λ - wavelength (nm)

a*P – TSS specific particulate absorption

a*PH – TChl-a specific phytoplankton absorption

a*Y – DOC specific CDOM absorption

aP - absorption coefficient of particles (1/m) measured by a laboratory spectrophotometer

aPH - absorption coefficient of phytoplankton (1/m) measured by a laboratory spectrophotometer

aPY – total absorption due to particy=ulate and dissolved substances

aY - absorption due to CDOM (1/m) measured by a laboratory spectrophotometer

Tchl-a – total Chlorophyll-a concentration

Contents

1 Introduction

Changes in water quality can significantly influence coastal aquatic ecosystem health (Haynes et al., 2007) and can impact socio-economic conditions of human populations that depend on coastal aquatic resources. Multiple factors can affect water quality, including sediment pollution, temperature, dissolved oxygen content, nutrient levels and the presence of contaminants (Brodie et al., 2017). Changes in water quality has consequences on various aspects of aquatic ecosystem (including productivity of regional aquaculture industry). Water quality directly affects the survival and reproduction of aquatic organisms. Fish, invertebrates, and plants have specific requirements for temperature, pH, dissolved oxygen, and nutrient levels. If these parameters deviate from their optimal range, it can lead to stress, reduced growth, impaired reproduction, and even death of the organisms. Good water quality is also essential to support a diverse range of species within an aquatic ecosystem. Since different species have different tolerances to environmental conditions, when water quality deteriorates, sensitive species may decline or disappear, leading to a loss of biodiversity (Brown et al., 2019). This can disrupt the balance of the ecosystem and negatively impact the food web.

The combined impact of long-term climate changes and human activities significantly affects coastal water quality, with interactions and amplifications resulting in complex and interconnected effects. These influences contribute to increased water temperatures, altered land to ocean outflows, sediment and nutrient pollution, eutrophication, and habitat loss (Whitehead et al., 2009). Elevated long-term temperatures affect gas solubility, including oxygen, leading to reduced dissolved oxygen levels and subsequent habitat loss and decreased productivity. Land and marine based activities such as agriculture and aquaculture are increasingly resulting in pollution from particulate and dissolved substances, ultimately leading to ecosystem eutrophication and degraded ecosystem health (Giri et al., 2016).

The conventional approach to coastal water quality sampling, which involves manual collection from boats, has limitations including limited spatial coverage, low temporal resolution, challenges in monitoring large-scale events, and high costs and resource requirements (Madrid et al., 2007). To address these limitations, alternative sampling methods have emerged, such as autonomous underwater vehicles, fixed monitoring stations and satellite remote sensing technologies (Dickey et al., 2006). These alternatives provide improved spatial coverage, higher temporal resolution, and the capability to collect data on multiple biogeochemical processes, enabling a more comprehensive understanding of coastal water quality.

Fixed monitoring stations offer numerous benefits for coastal observations due to their continuous monitoring capabilities. The uninterrupted data collection of water quality parameters facilitates a comprehensive understanding of long-term changes and trends in coastal water quality, including the detection of short-term fluctuations, diurnal patterns, and episodic events that can have significant impacts on coastal ecosystems (Antoine et al. 2008). The provision of data in real or near real time can provide information to marine users needed optimise operational activities and to protect of the marine environment. However, it is important to note that fixed monitoring stations have limitations in explaining large-scale biogeochemical connections within the ecosystem. This is an area where satellite observations of water quality parameters can provide valuable insights.

Satellite remote sensing offers numerous advantages for the study of coastal aquatic ecosystems and water quality. It enables the collection of ocean colour data over expansive areas, providing a comprehensive understanding of coastal and open ocean regions (Mouw et al., 2015). By retrieving multiple water quality parameters simultaneously, ocean colour remote sensing provides valuable insights into ecosystem health, primary productivity, nutrient dynamics, and the distribution of harmful algal blooms. Moreover, satellite-based remote sensing data is easily accessible worldwide, making it a cost-effective approach for monitoring and studying water quality parameters across vast marine areas. However, the primary limitation of satellite remote sensing for water quality assessment is the limited availability of high temporal resolution data, which is currently restricted to near-equatorial regions through geostationary satellites (Patricio-Valerio ET AL., 2022). To address this limitation, an integrated approach that combines high temporal resolution fixed station data with the broad spatial coverage of satellite ocean colour remote sensing is being employed in AquaWatch Australia Mission Figure 1).

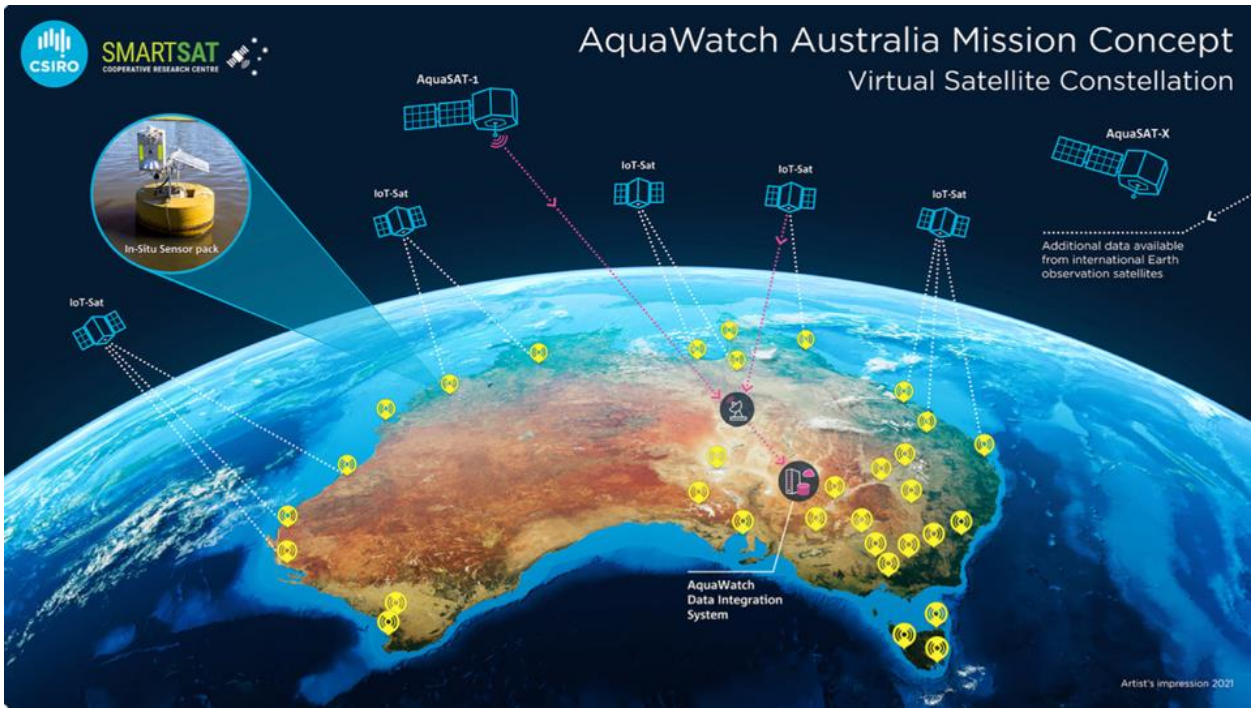

FIGURE 1: AQUAWATCH AUSTRALIA MISSION CONCEPT

To address the challenge of integrated information for coastal water quality monitoring in support of Aquaculture operations, this collaborative project has the following objectives:

1. Develop and deploy a fixed monitoring station along the coast equipped with both above and underwater sensors to continuously monitor water quality changes at a high temporal resolution.
2. Implement ocean colour water quality algorithms to analyze and monitor changes in water quality using high spatial resolution LandSat-8 satellite data.
3. Demonstrate the integration of in-situ and satellite water quality observations on the AquaWatch data integration and analytics (ADIAS) platform.

The integration of multi-sensor data on an AquaWatch ADIAS platform (also known as EASI AquaWatch - https://research.csiro.au/cceo/underpinning-technologies/earth-analytics/) is anticipated to offer convenient access to analysis-ready data, improving our comprehension of biogeochemical connections in coastal waters and facilitating a more precise interpretation of coastal ecosystem health through fine-resolution monitoring and trend analysis. This integrated approach establishes a comprehensive and robust framework for monitoring coastal water quality and managing ecosystems effectively.

2 Study Area

The implemented earth observation integration project focuses on Boston Bay in South Australia. Boston bay is located in the southwestern corner of Spencer Gulf on the eastern side of the Great Australian Bight (Figure 2). Providing a natural harbour for regional city of Port Lincoln, commonly referred to as the "Seafood Capital of Australia", Boston Bay and adjoining embayments hosts South Australia's most diverse, valuable, and productive aquaculture zones. In 2019/20 it was estimated approximately 13,150 tonnes of aquaculture seafood, including Southern Bluefin Tuna, Yellowtail Kingfish and Blue Mussels, with a total value $180 M was produced from this region (BDO EconSearch, 2020; https://www.bdo.com.au/en-au/insights/advisory/econsearch-en/south-australian-commercial-fisheries-reports).

In terms of oceanography, Boston Bay and its surrounding embayment are directly connected Spencer Gulf and functions as a sub-basin within the gulf. Connectivity with shelf waters of the eastern Great Australian Bight is greatest during autumn and winter periods because of the gulfs inverse estuarine circulation (Nunes vaz et al. 1990). This facilitates and inflow water and nutrients from the shelf at a time when local anthropogenic nutrient inputs are greatest resulting in a peak in phytoplankton productivity and biomass (Middleton et al. 2013; Tanner et al., 2020).

Boston Bay experiences large variations in temperature and salinity (Middleton et al. 2013; Doubell and James 2023) resulting from strong seasonal changes in heating, evaporation, and episodic freshwater inflows from stormwater and the Tod River (Gaylard 2009). Water temperatures range between approximately 12 and 24 °C between summer and winter and coincide with annual salinity changes of approximately 1.4 PSU (Doubell and James 2023). In addition, currents generated predominantly by tides and wind, result in the reduced flushing of the bays inshore waters relative to the adjacent offshore waters of Spencer Gulf (Herzfeld et al., 2009; Middleton et al., 2013, 2014).

Ultimately, variations in regions unique physical, chemical and biological oceanographic components interact and influence the water quality experienced in the bay. Considering the importance of aquaculture to the local and South Australian economy, there is a need to improve water quality monitoring to improve the sustainability and development of aquaculture in the region and protect the overall health and ecology of the receiving marine ecosystem (Roberts et al., 2019; Tanner at al. 2020).

(A)

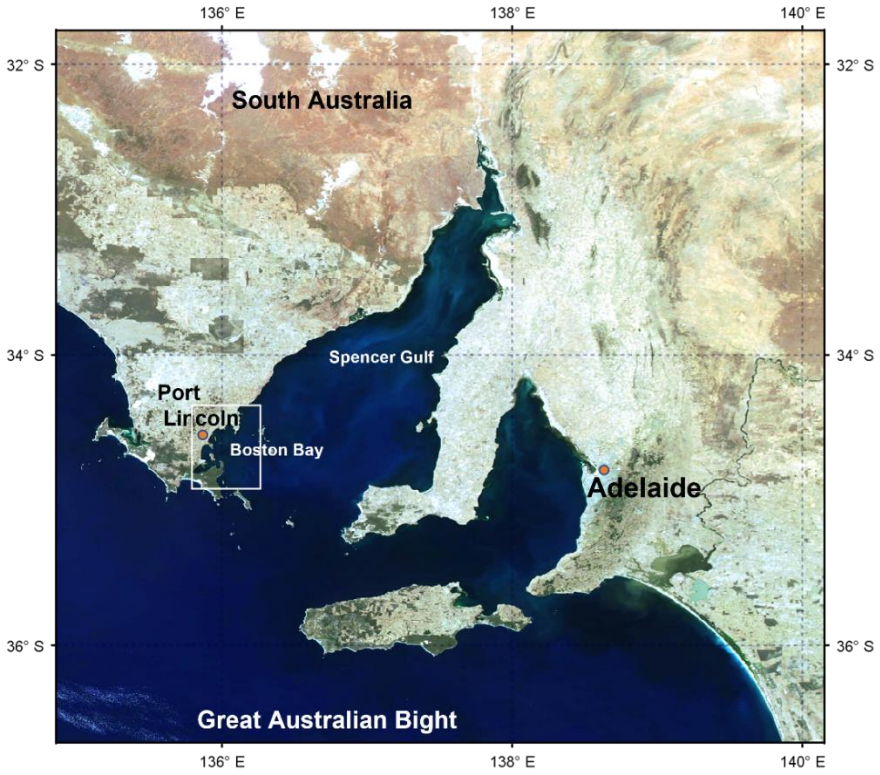

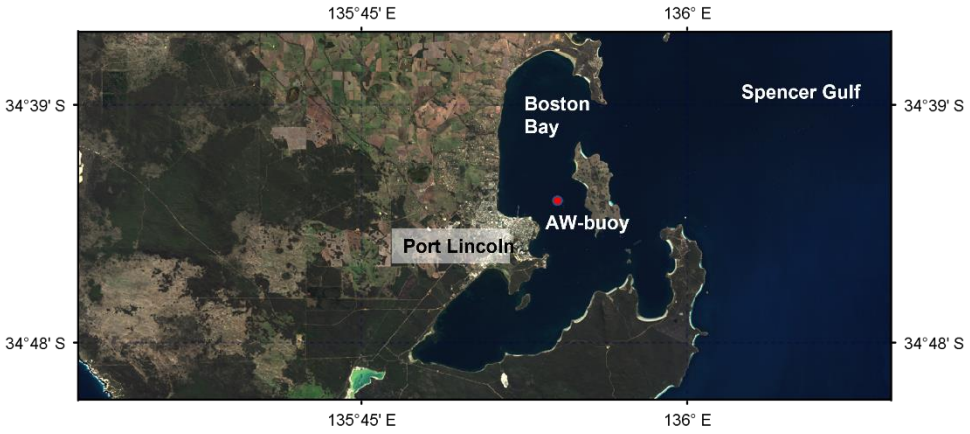

(B)

FIGURE 2 STUDY REGION. (A) MODIS AQUA IMAGE FROM 19/FEB/2023 SHOWS THE LOCATION OF SPENCER GULF REGION, AND (B) LANDSAT-8 IMAGE FROM 22/APRIL/2023. RED COLOUR MARKER INDICATES THE LOCATION OF AQUAWATCH BUOY IN BOSTON BAY.

3 Project Results

3.1 Project Design

Water quality is of utmost importance in coastal aquaculture sites, directly impacting the well-being of aquatic organisms and the overall success of aquaculture operations. Maintaining good water quality is crucial for the health, growth, and reproduction of cultured species. Water serves as a vital source of

oxygen for respiration, carries essential nutrients for growth, and facilitates the removal of metabolic waste products. Conversely, poor water quality can lead to stress, disease, and even mortality among cultured organisms.

The rate at which hypoxia develops in coastal waters can vary based on factors such as water body conditions, nutrient inputs, temperature, and circulation patterns. Hypoxia typically takes hours to days to develop and can persist for longer periods depending on the circumstances. Monitoring dissolved oxygen (DO) levels and ensuring sufficient aeration are vital for preserving optimal water quality in aquaculture sites.

Eutrophication poses another significant challenge in aquaculture sites, referring to the excessive enrichment of water bodies with nutrients that promote increased algal growth. Harmful algal blooms (HABs) can develop in coastal waters within days to weeks, influenced by various factors including algal species, environmental conditions, nutrient availability, and water circulation patterns (Roberts et al., 2019).

To establish an effective water quality monitoring and management program, it is necessary to monitor multiple parameters at different time scales. Relying on a single method of observation, such as *in situ* or satellite-based monitoring, is insufficient for a holistic understanding of water quality dynamics.

To overcome this challenge, integrating multiple data streams from *in situ* and satellite platforms is the most viable option. By combining information from various sources, the accuracy and reliability of water quality assessments can be enhanced. In situ monitoring provides detailed insights into specific areas, while satellite-based monitoring offers broader coverage over larger areas, providing a comprehensive understanding of water quality patterns and trends.

Integrating these data streams allows for a more comprehensive assessment of water quality parameters, enabling informed decision-making and effective management practices. Strategies such as installing bio-optical buoys with sensors, collecting and processing satellite observations, and integrating *in situ* and remote sensing data on a unified platform are pursued to achieve the objective of integrated data delivery.

By implementing these measures, the project aims to combine data from different sources and provide a cohesive data delivery system (as illustrated in Figure 3). This integrated approach enhances the accuracy, completeness, and accessibility of water quality data, supporting informed decision-making and effective management practices in water quality monitoring and management programs.

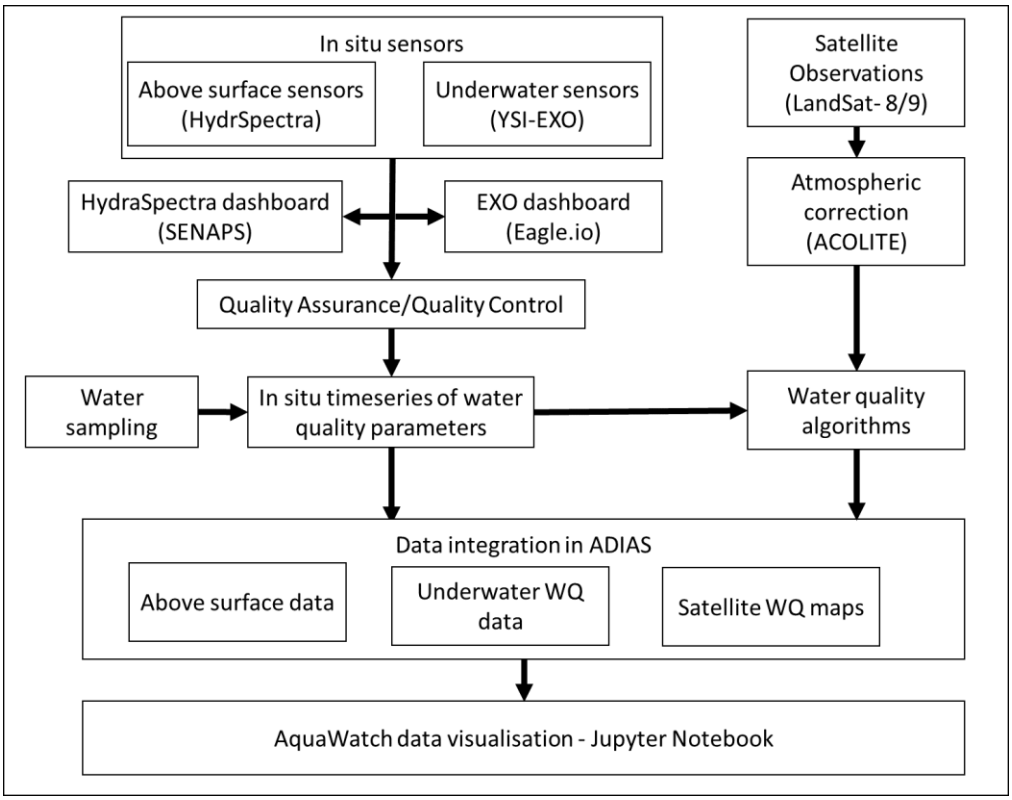

FIGURE 3 AQUAWATCH IMPLEMENTATION OF INTEGRATED DATA SYSTEM IN SPENCER GULF PROJECT. IN SITU SENSORS WERE INSTALLED IN BOSTON BAY REGION WITH HELP FROM PROJECT PARTNERS (SARDI).

The study site underwent a selection process to identify and install appropriate underwater sensors suitable for coastal deployment (project deliverables, D1 and D2; see Table A1 in Appendix). Following their installation, the sensor data were regularly compared with water samples collected at the buoy site. To ensure the accuracy and reliability of the sensor measurements, researchers from SARDI conducted regular field trips to maintain the instruments and collected water samples for testing and comparing against the sensor data (deliverable, D3).

The data collected from the sensors and water samples underwent iterative processing and integration steps to achieve deliverables 4 and 5. These steps involved refining and analyzing the data to extract meaningful information and insights. The details of deliverables 2-5, including the methodology and outcomes, can be found in the respective sections below, providing a comprehensive understanding of the project's progress and results.

In summary, the project design (deliverable: D1) now enables the collection of multiple water quality parameters in the study region. The implemented methodology and processing chains have resulted in the creation of a single platform that integrates both *in situ* and satellite observations of water quality parameters. This integrated platform provides easily accessible, analysis-ready water quality observations. It is expected that this availability of timely and reliable water quality data will facilitate effective monitoring and management of the ecosystem in the Boston Bay region of Spencer Gulf.

4 Sensor selection, buoy design and test plan

4.1 Site selection

The process of selecting the site involved extensive consultation with our project partners at SARDI (Tanner et al 2020), to ensure a well-informed decision. After thorough evaluation, the highlighted site (Figure 4) was chosen as the AquaWatch Pilot project site due to its fulfillment of essential requirements. The selection was based on several factors, including:

- Sufficient water depth of approximately 16 meters, which minimized the interference caused by reflected light from the sea bottom, ensuring accurate measurement of water reflectance using EO technology.
- Relatively calm water conditions, providing a stable environment for monitoring and data collection.
- Avoidance of significant ship traffic in the vicinity, minimizing potential disturbances and ensuring uninterrupted operations.
- Proximity to an existing SA water mooring site, facilitating logistical convenience and access to necessary infrastructure.
- Adjacency to aquaculture facilities (such as kingfish and tuna fish pens), enabling close monitoring and assessment of the surrounding aquatic environment.
- Integration of data into SARDI's existing hydrodynamic models, enhancing the accuracy and reliability of the collected information.
- Promising potential for future expansion to additional sites, allowing for the scalability and broader application of the AquaWatch project.

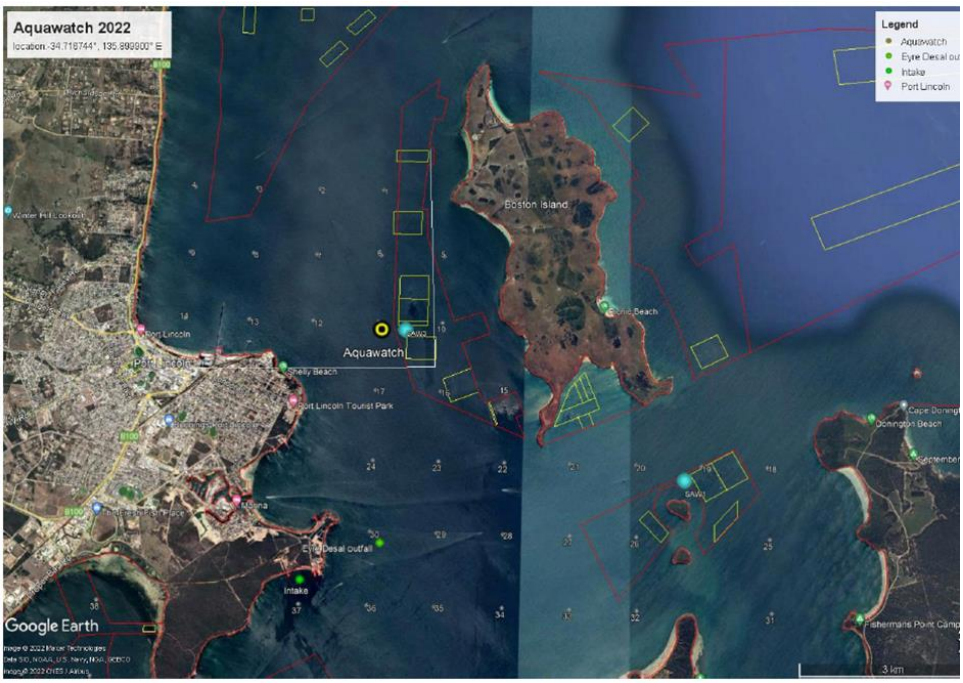

FIGURE 4 MAP OF THE SPENCER GULF AND THE SITE SELECTED FOR AQUAWATCH MONITORING STATION, INDICATED BY A YELLOW CIRCLE. AQUA-BLUE DOTS REPRESENT THE EXISTING FOOTPRINT OF SARDI'S MOORING LOCATIONS FROM PROJECT WORK WITH SA WATER (SA GOV WATER AGENCY) AND RED AND YELLOW LINES, REPRESENTING LOCAL AQUACULTURE LEASE SITES.

4.2 Sensor selection

The ground *in situ* sensors are critical for the AquaWatch mission as they provide necessary calibration/validation of earth observation data. Additionally, they offer complementary information that cannot be derived from Earth Observation data and guide representative water sampling. A suite of above and below-water sensors were proposed to validate water reflectance derived from the satellite observations using visible and/or near-infrared spectral bands.

To satisfy the above requirement, the HydraSpectra sensor was proposed as the above water sensor. The HydraSpectra, developed by CSIRO, is a low-cost optical system designed for field-deployed water quality monitoring of water bodies based on spectral reflectance. This sensor captures data that can be used to estimate chlorophyll, Coloured Dissolved Organic Matter (CDOM), and Total Suspended Solids (TSS) concentrations with accuracy comparable to other research spectroscopic systems.

For the in-water sensors, there was a need to monitor several water quality parameters, including temperature, salinity, turbidity, dissolved oxygen, pH, chlorophyll, phycoerythrin (TAL-PE), CDOM (Coloured Dissolved Organic Matter), and optional nutrient levels. After reviewing over 30 water quality sensor suppliers in terms of sensor sensitivity, selectivity, stability and dynamic range and also considering system compatibility with existing pilot projects, it was decided to choose Xylem YSI 's multiparameter sonde (https://www.ysi.com/exo2) to monitor multiple water quality parameters simultaneously.

SARDI also provided JFE's HAI (Harmful Algal Indication) Sensor, a harmful plankton detector (https://www.jfe-advantech.co.jp/eng/products/ocean-haisensor.html). This sensor is specifically designed to identify two phytoplankton species known for causing harmful blooms: *Karenia mikimotoi* and *Chattonella antiqua*. The HAI instrument calculates the ratio of fluorescence intensity at 690 nm to that at 670 nm, defined as the Fluorescence Spectral Shift Index (FSI). This FSI value serves as a quick assessment tool to determine the occurrence risk of Harmful Algal Blooms.

4.3 System design

The monitoring station consists of a buoy platform equipped with a variety of integrated instruments and devices (Figure 5). The selection of buoys was based on the specific sea conditions in the region, taking into account factors such as significant waves, strong winds, and expansive open waters. To ensure precise reflectance measurements for the Hydraspetra sensor, it was crucial to have a highly stable platform. As a result, the Xylem DB1750 buoy was chosen to meet the stability requirements. To further minimize buoy rotation, a dual anchor design was implemented.

The buoy platform integrates multiple instruments and devices, including three sensors, a power supply module, a data logging and telemetry module, and a weather station. Power is provided to all three sensors and the weather station using a Power Sonic 70AH rechargeable deep cycle battery. To charge the battery during daylight hours, three solar panels connected in parallel are linked to a Sunsaver10 solar charge controller. This setup eliminates the need for the battery and solar panel that come with the Hydraspetra sensor, reducing redundancy in the system.

For data logging and telemetry, both the Sonde and the HAB sensor are connected to a Campbell Scientific CR1000X programmable data logger. This data logger is further connected to a DualMAX MA2055 3G/4G modem, enabling wireless transmission of sensor data. The Hydraspetra sensor has

separate data acquisition and telemetry modules. Additionally, a Gill weather station, a Garmin GPS, and a sea light have been installed on top of the buoy.

FIGURE 5 DESIGN OF THE MONITORING STATION.

4.4 System installation

On August 31st, 2022, the above system was successfully deployed in Boston Bay, situated within Spencer Gulf (34° 43.538’ S, 135° 54.156’ E). The installation was accomplished with the support of SARDI's research vessel, RV Ngerin (Figure 6).

The buoy was dual anchored, and oriented to the north, which mostly prevents rotation, but some rotation may affect the quality of the HydraSpectra reflectance measurement, therefore the tilt of the buoy is recorded in real-time to monitor the buoy movement.

The HydraSpectra, the MKIII model, comprises a camera, an electronic control box, and a solar panel (30 w). The sensor transmits approximately 5GB of data per month; a SIM card (Telstra) with a 60 GB data allowance was inserted into the instrument to ensure sufficient data backup space. The sensor head was secured on an aluminium pole mounted onto the circular steel grab rail on the DWER buoy with U-bolts. This placed the HydraSpectra sensor approximately 1m above the water surface. The sensor head was levelled ensuring a clear Field of View (FOV) facing the optimal southeast orientation to minimise

specular reflection and forward scattering of sunlight into the optical apertures. All external cables were placed into flexible split conduits and secured to the pole with cable ties to reduce the risk of damage. To prevent birds from perching on the camera, bird spikes were fitted on top of the HydraSpectra sensor.

The in-water sensors, namely the multiparameter sonde and the HAI sensor, were installed through the moon pool of the buoy and suspended at approximately 0.6 meters depth in the water.

Figure 6 . DEPLOYMENT OF THE IN SITU MONITORING STATION, SARDI RV NGERIN.

Metadata information, including the site name, site GPS coordinates, timestamp (including time zone), unit bearing, sensor height above the water, photos taken during deployment, and other field notes such as additional sensors installed, were recorded.

The status of all sensors was closely monitored to identify any issues following the deployment.

To monitor the water quality data in near real-time, the HydraSpectra live data streams are sent to the CSIRO ftp server and then ingested into the CSIRO Senaps IoT platform. This platform is also responsible for conducting image processing of the raw images acquired by the sensor and generating reflectance spectra. Additionally, the Eagle.io platform is utilized to upload and visualize data from all other integrated water quality sensors.

Monitoring the system's status is essential to ensure its effective operation, and we can easily do this by creating the dashboard for the *in situ* monitoring station (Figure 7). This will allow us to check the sensor data acquired, battery voltage and cable current for effective power management. Moreover, we have the capability to remotely control the sensors, which allows us to adjust the sampling rate, switch the system on and off, and manually acquire data as needed. This remote-control capability provides us

with increased flexibility and allows us to tailor the system's operation to the specific needs of the AquaWatch Mission.

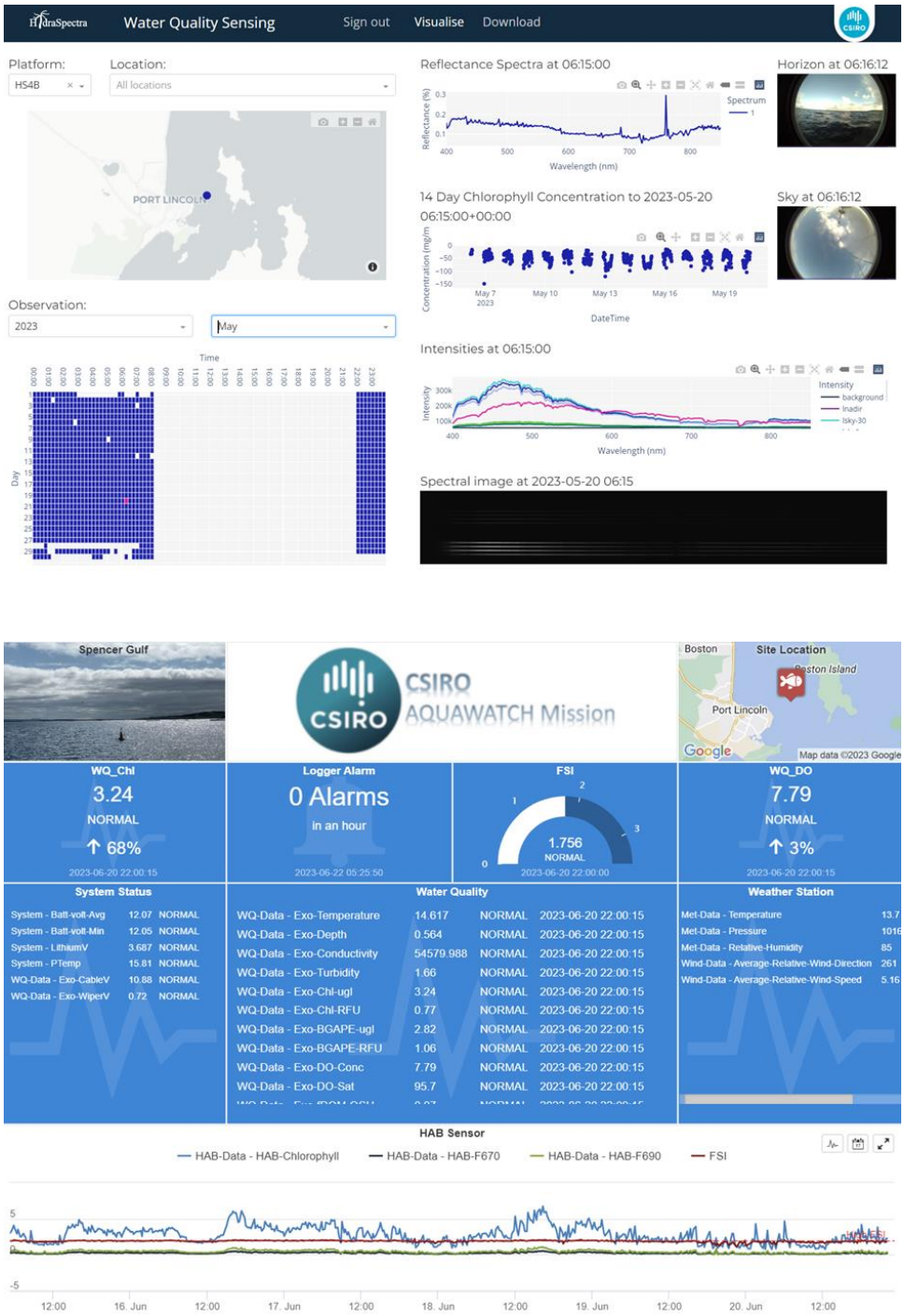

FIGURE 7 DASHBOARDS FOR MONITORING PERFORMANCE OF THE *IN SITU* SYSTEM. TOP: HYDRASPECTRA, BOTTOM: IN WATER SENSORS

For routine cleaning and maintenance of the system, SARDI took the responsibility to conduct routine maintenance of the system which include cleaning the HydraSpectra and replacing the in-water probes with calibrated probes and water sample collection on a bi-monthly basis.

4.5 ADIAS Platform and In-situ data ingestion

ADIAS is a cloud-based data warehouse and analysis platform implemented for the AquaWatch mission. ADIAS provides scientists with a configurable development environment to ingest, track, process and analyse a diverse array of data. For this project ADIAS provided a single platform where data from in-water, HydraSpectra and remote sensing data could be housed, quality controlled and analysed. The purpose built datalake used to house the *in situ* data is described below, for a discussion of remote sensing data see 5.1.3.

To improve the ease of use of sensor data streamed from the HydraSpectra and various in water sensors deployed in the field, the in-situ data pipeline is designed to manage credentials and configuration in the AWS cloud, implement multiple platform specific integrations and regularly poll the IoT platforms to consolidate the data in a purpose built datalake in AWS. This datalake is then queryable from the science experimentation platform - ADIAS using a single consistent SQL (database query language) interface. This pattern homogenises data access, abstracts away platform specific complexity and improves security by managing the access credentials in a single place instead of distributing them among team members.

By leveraging the in-situ data pipeline, scientists can easily access real-time data from sensors without the need to learn multiple technical interfaces associated with Internet of Things (IoT) platforms. In the AWS cloud, a data pipeline efficiently organizes the data, converting it into a user-friendly format such as a pandas or dask dataframe. This streamlined format allows for easy analysis in a notebook, facilitating experimentation in conjunction with earth observation data.

4.6 In-situ data QA/QC

QA/QC of the HydraSpectra data:

The accuracy and precision of spectral reflectance measurements conducted in the field can be influenced by various factors, including environmental conditions, viewing geometry, light illumination changes including time of day, and instrument calibration (Zibordi et al., 2015, Toole et al., 2000, Mobley et al., 1999, Pfitzner et al., 2011). The full systematic workflow for quality control of HydraSpectra reflectance measurements is currently under development. To mitigate the influence of changing illumination conditions, we specifically chose data collected between 11:30 am and 13:30 pm for analysis. Furthermore, we are actively working on developing additional data processing steps to achieve a thorough quality assurance of HydraSpectra data streams. These include:

- Evaluating the impact of variations in viewing geometry, such as tilt angles
- Correcting for the spectral effects of neutral density filters and diffusers integrated into the instrument
- Excluding measurements affected by the shadow cast and other influences induced by low sun angles
- Calculation of the degree of cloud cover from on-board camera data
- Correcting for residual surface sun glint
- Quantifying spectrum noise and measures to reduce its impact

QA/QC for water quality sensors:

QA/QC for water quality sensors is essential for ensuring accurate and reliable water quality data. Through rigorous QA/QC protocols, we can confidently assess the health and safety of water resources,

enabling informed decision-making and effective water management strategies. Additionally, accurate and consistent water quality data obtained through QA/QC measures facilitates the matching of in-situ data with remote sensing data, supporting remote sensing calibration and validation efforts.

During the project, a graphical inspection of the collected data revealed several anomalies, including out of range values, missing values, duplicate values, spikes, outliers, sensor signal drift, and noisy signals. It is essential to determine the causes of these anomalies, distinguishing between those resulting from environmental variations and those likely caused by sensor malfunctions, calibration events, or fouling. Identifying the causes of sensor data anomalies helps plan operations, make informed decisions, conduct sensor inspections, and issue environmental warnings.

The sensor data correction process involves several steps: range check, spike removal, sensor drift correction, missing data interpolation, and sensor data smoothing. These steps were applied to process the Chlorophyll, Turbidity, and fDOM sensor data. The comparison between the raw Chlorophyll sensor data and the processed data is presented in the following chart (Figure 8).

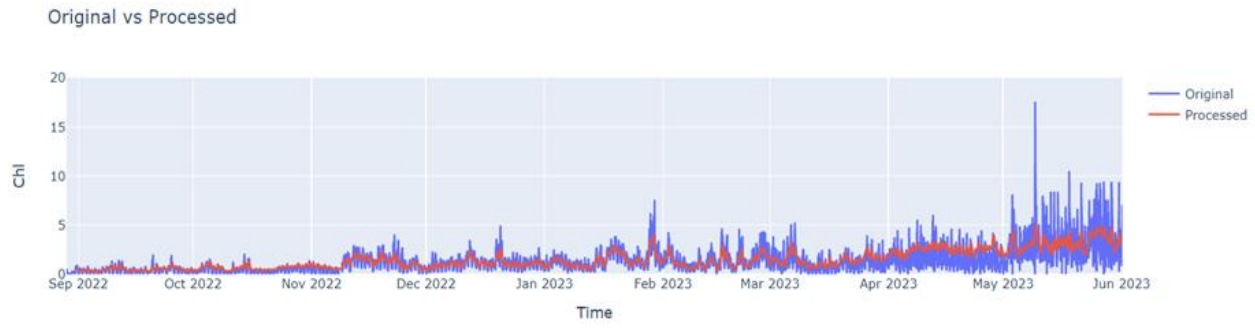

Figure 8 . THE RAW CHLOROPHYLL SENSOR DATA AND THE PROCESSED DATA

Moving forward, it is recommended to extract characteristic features related to anomalies and perform automated anomaly detection and correction to increase data processing efficiency dealing with large quantities of *in situ* data (Morello et al 2014, Liu et al 2004).

4.7 Bio-optics of the region

Bio-optical measurement methods: During bi-monthly maintenance visits in Boston Bay, water samples were collected in the vicinity (0 - 2 km radius) of the AquaWatch buoy. Upon reaching the buoy location, surface water was carefully collected using a clean plastic container. Shortly after retrieval, the water was filtered, and the filtered samples were appropriately stored for subsequent biogeophysical measurements in the laboratory, as described in Tilstone et al., (2004). To separate the Total Suspended Solids (TSS), up to 3 liters of seawater was passed through a glass fiber filter with a pore size of 0.7 mm (Whatman GF/F). The filters containing the suspended solids were then stored in a cool and dark environment until further analysis. To determine the TSS concentration in milligrams per liter (mg/L), the filters were dried at 60 °C until a constant weight was achieved. For the analysis of suspended particulate inorganic matter (SPIM), the filters underwent additional processing. They were subjected to drying at 450 °C for a duration of 3 hours. This procedure aimed to derive the concentration of SPIM in

the samples. By calculating the difference between the TSS and SPIM concentrations, the concentration of Suspended Particulate Organic Matter (SPOM) could be determined.

To analyze phytoplankton pigments, a specific volume of sample water (ranging from 0.1 to 3 liters) was collected from the surface and passed through a 25 mm Whatman GF/F glass-fiber filter. Subsequently, the filters were carefully stored in cryovials immersed in liquid nitrogen until the analysis. For pigment analysis, the filters were extracted and subjected to High-Performance Liquid Chromatography (HPLC) using a Waters-Alliance system. The detailed protocol for this analysis can be found in Clementson (2012). Total chlorophyll a (TChla) was calculated by combining the amounts of monovinyl- and divinyl-chlorophyll a, as well as chlorophyll-a allomers and epimers. To determine the dissolved organic carbon (DOC) content, seawater was filtered using a Whatman ANODISC filter with a pore size of 0.2 µm. Prior to filtration, the filter was rinsed with Milli-Q water. The resulting filtrate was transferred to a bottle that had been pre-rinsed with the same filtered seawater and then acidified with 0.5 ml of 50% H_3PO_4. The acidified filtrate was stored in a refrigerator at 2–4 °C according to Ferrari (2000). Upon arrival at the laboratory, the DOC measurements were conducted using a Formacs HT Combustion TOC Analyzer manufactured by Skalar. This analyzer employs the combustion method and offers accuracy up to 1 mg/L of organic carbon.

The particulate absorption coefficient, encompassing both phytoplankton and nonalgal components, was determined through the following procedure. Surface water samples (ranging from 0.1 to 3 liters) were collected and filtered using a 25 mm Whatman GF/F glass-fiber filter. These filters were then stored flat in liquid nitrogen until further analysis. To assess the optical density of the overall particulate matter, measurements were taken across the spectral range of 250–800 nm, with 0.9 nm increments. This was accomplished using a Cintra 404 UV/VIS dual beam spectrophotometer equipped with an integrating sphere. For the determination of optical density associated with nonalgal matter, pigmented material was extracted from the sample filter using the method described by Kishino et al. (1985). By calculating the difference between the total particulate matter and the optical densities of nonalgal particulate matter (across the entire spectral range), the optical density attributed to phytoplankton was obtained. To calculate the absorption coefficients, the pathlength amplification correction method by Mitchell B (1990) was employed. In addition to the particulate absorption coefficient, the absorption coefficient due to colored dissolved organic matter (CDOM) was also measured. Sample water was filtered through a 0.22 µm filter (Whatman ANODISC), and the filtrate was stored in glass bottles, kept in the dark at 4 °C until analysis immediately after the field survey. The CDOM absorbance of the filtrate was measured using a Cintra 404 UV/VIS spectrophotometer with a 10 cm pathlength quartz cell. Fresh Milli-Q water served as a reference during the measurements. To normalize the absorption coefficient, it was set to zero at 680 nm.

Bio-optics analysis: Historical records for Boston Bay do not include bio-optical data obtained from water samples. However, this project managed to collect a limited amount of bio-optical data, providing some insights into the distribution of bio-optical parameters in the region. The primary aim of collecting bio-optical data in this project was to compare conventional lab-based measurements with in-situ sensor measurements. Additionally, these bio-optical measurements are expected to enhance our understanding of the bio-optical characteristics of the waters in Boston Bay. It is important to note that the available bio-optical measurements are limited in scope. Therefore, this study does not seek to present a comprehensive bio-optical analysis. Rather, its objective is to provide a preliminary exploration of the bio-optical properties in the area.

In Boston Bay, the levels of Total Suspended Sediment (TSS) are generally observed to be quite low. These TSS values are comparable to estimates found in open ocean waters, such as those in the east Australian current waters as documented by Cherukuru et al. (2017). The suspended sediment in the bay primarily comprises organic particulate matter, with mean values of Suspended Particulate Organic Matter (SPOM) exceeding 60%. The total Chlorophyll-a (Tchl-a) concentrations in the waters of Boston Bay exhibit ranges and mean values (as presented in Table 1 and Fig 8 A) that are similar to measurements recorded in other temperate regions of Australia. However, there is a notable variation in the range of Tchl-a concentrations between the months of August and November, suggesting a significant temporal shift in this parameter during that period.

Phytoplankton pigment measurements in Boston Bay have revealed an intriguing shift in the phytoplankton community. Certain pigments are specific to phytoplankton groups, making them "diagnostic pigments" (e.g., fucoxanthin for diatoms, peridinin for dinoflagellates, zeaxanthin for cyanobacteria) as described by Bricaud (2004). The analysis of pigment data using High-Performance Liquid Chromatography (HPLC) (depicted in Fig 3.3.x B) indicates that in August, there is a comparable presence of diatoms (fucoxanthin), haptophytes (hex-fuco), and chlorophytes (Chl-b) in Boston Bay waters. However, by November/2022, the dominance shifts primarily to diatoms, as evidenced by the increased abundance of Fucoxanthin. The variability of dissolved organic carbon (DOC) in Boston Bay corresponds to that observed in other temperate Australian waters with minimal inputs from land-based sources. At the sampling site, short-term fluctuations in DOC during November 2022 and February 2023 were measured to be 28.4% and 10.8%, respectively, as shown in Table 1.

Table 1: Variability of biogeochemical properties of waters surrounding the AquaWatch buoy in Boston Bay, Spencer Gulf.

	August, 2022	November, 2022	February, 2022
Parameters	Min – Max, Mean (CV%)	Min – Max, Mean (CV%)	Min – Max, Mean (CV%)
TSS (mg/L)	Data not available	0.87 -1.13, 0.99 (9.9)	1.0 -1.43, 1.22 (12.6)
SPOM (%)	Data not available	55.9 -79.1, 64.1 (14.7)	54.7 – 81.9, 68.6 (14.1)
Tchl-a (µg/L)	0.34 – 0.41, 0.37 (8.8)	0.38 – 0.74, 0.56 (24.6)	Data not available
DOC (mg/L)	Data not available	1.6 – 2.8, 1.9 (28.4)	1.9 -2.4, 2.1 (10.8)

(A)

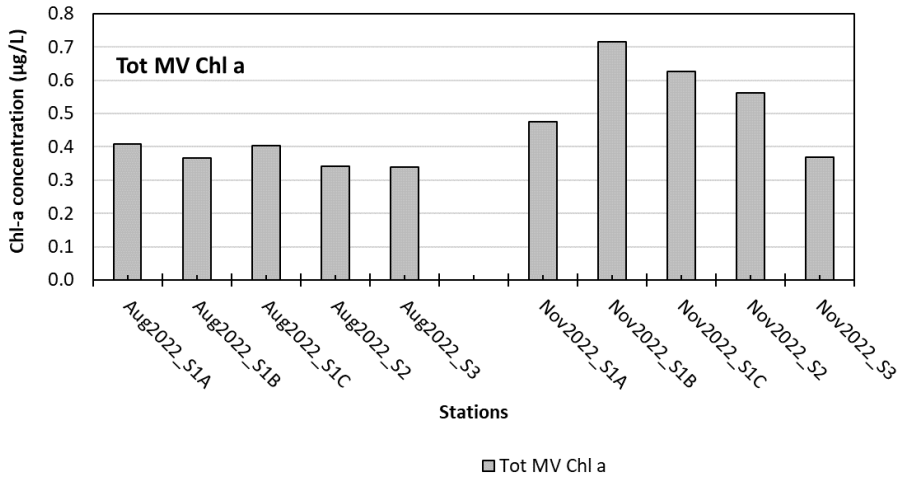

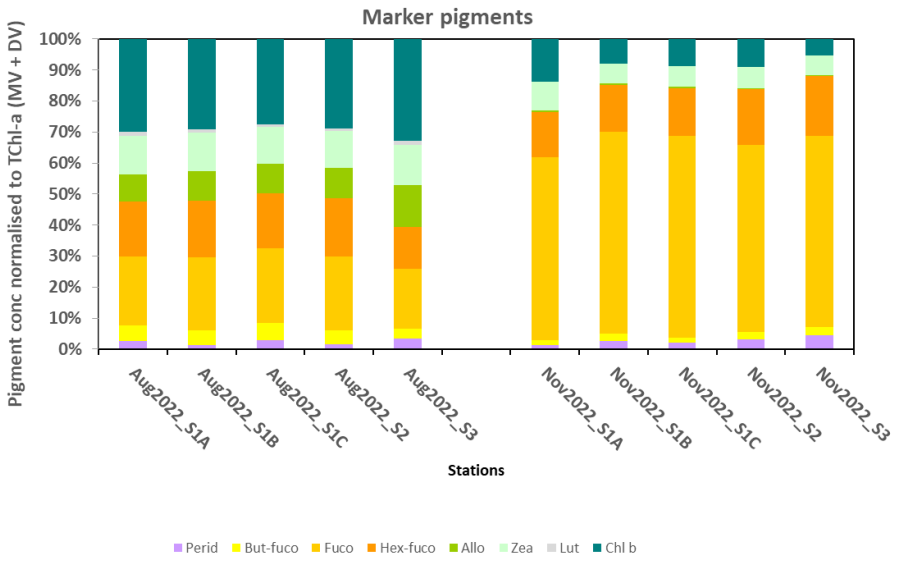

(B)

FIGURE 9 PHYTOPLANKTON PIGMENT DISTRIBUTIONS IN WATERS ADJACENT TO AQUAWATCH BUOY IN BOSTON BAY, SPENCER GULF.

Absorption properties: The presence of phytoplankton, non-algal particulate matter (NAP), and coloured dissolved organic matter (CDOM) affects the way light is absorbed in the water and influences the remote sensing reflectance signature (Lee et al., 2004). The total spectral light absorption coefficient of natural waters (aT) encompasses the absorption by optically active particulate and dissolved substances in the water ($aT(\lambda) = aW(\lambda) + aP(\lambda) + aY(\lambda)$), including contributions from water (aW), particulate matter (aP), and CDOM (aY). Particulate matter is further divided into contributions from phytoplankton and non-algal particulate matter ($aP(\lambda) = aPH(\lambda) + aNAP(\lambda)$) [Cherukuru et al., 2020]. For the purposes of this study, the spectral range considered is λ = 400–700 nm.

The colour of the ocean in Boston Bay is largely influenced by the absorption of light by phytoplankton. Specifically, the presence of chlorophyll-a pigments results in two distinct absorption peaks, approximately at 440 and 676 nm. Changes in chlorophyll-a concentrations lead to variations in phytoplankton absorption, which can be quantified using the relationship aPH(676) = 0.023[Tchl-a]^1.1, with an R-squared value of 0.85. Notably, the contribution of phytoplankton absorption to the total absorption by particulate matter is higher in the red region of the spectrum compared to the blue and green regions. In addition to phytoplankton, the absorption of light by non-algal particulate matter (NAP) also plays a role in determining the ocean's colour. NAP absorption is more

prominent in the blue region of the spectrum and gradually decreases exponentially towards the red part of the spectrum (Figure 10). Compared to phytoplankton, NAP is the dominant component responsible for light absorption across the blue, green, and red regions, with average percentage contributions of 57%, 82%, and 47%, respectively.

Coloured dissolved organic matter (CDOM) is another significant component present in the ocean's dissolved organic carbon (DOC) pool, contributing to its optical signature. CDOM absorption decreases exponentially with increasing wavelength. Notably, in Boston Bay, the absorption values attributed to CDOM are relatively higher compared to the absorption by particulate matter.

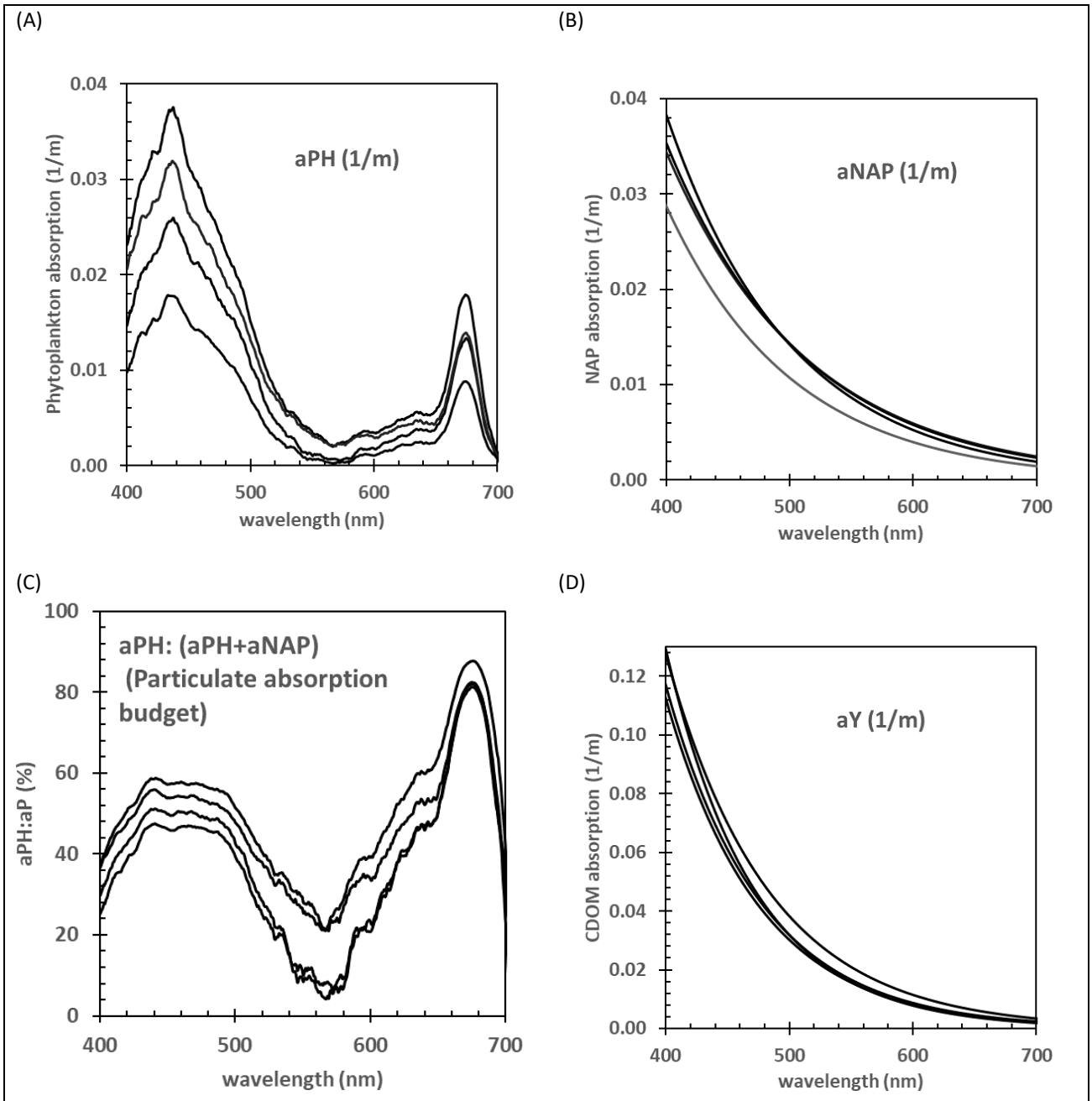

FIGURE 10 VARIABILITY IN LIGHT ABSORPTION DUE TO PARTICULATE AND DISSOLVED SUBSTANCES.

The absorption budget refers to the proportionate contributions of phytoplankton, nonalgal particles, and CDOM (Coloured Dissolved Organic Matter) to the absorption coefficient. It provides insights into the primary contributors to the absorption coefficient in the surface layer. Analysis of light absorption budgets in Boston Bay

reveals that CDOM plays a dominant role in light absorption within these waters (Figure 11). Phytoplankton's significant contribution is limited to the red region of the spectrum, while in the rest of the spectrum, its contribution is low and is like that of nonalgal particles (NAP).

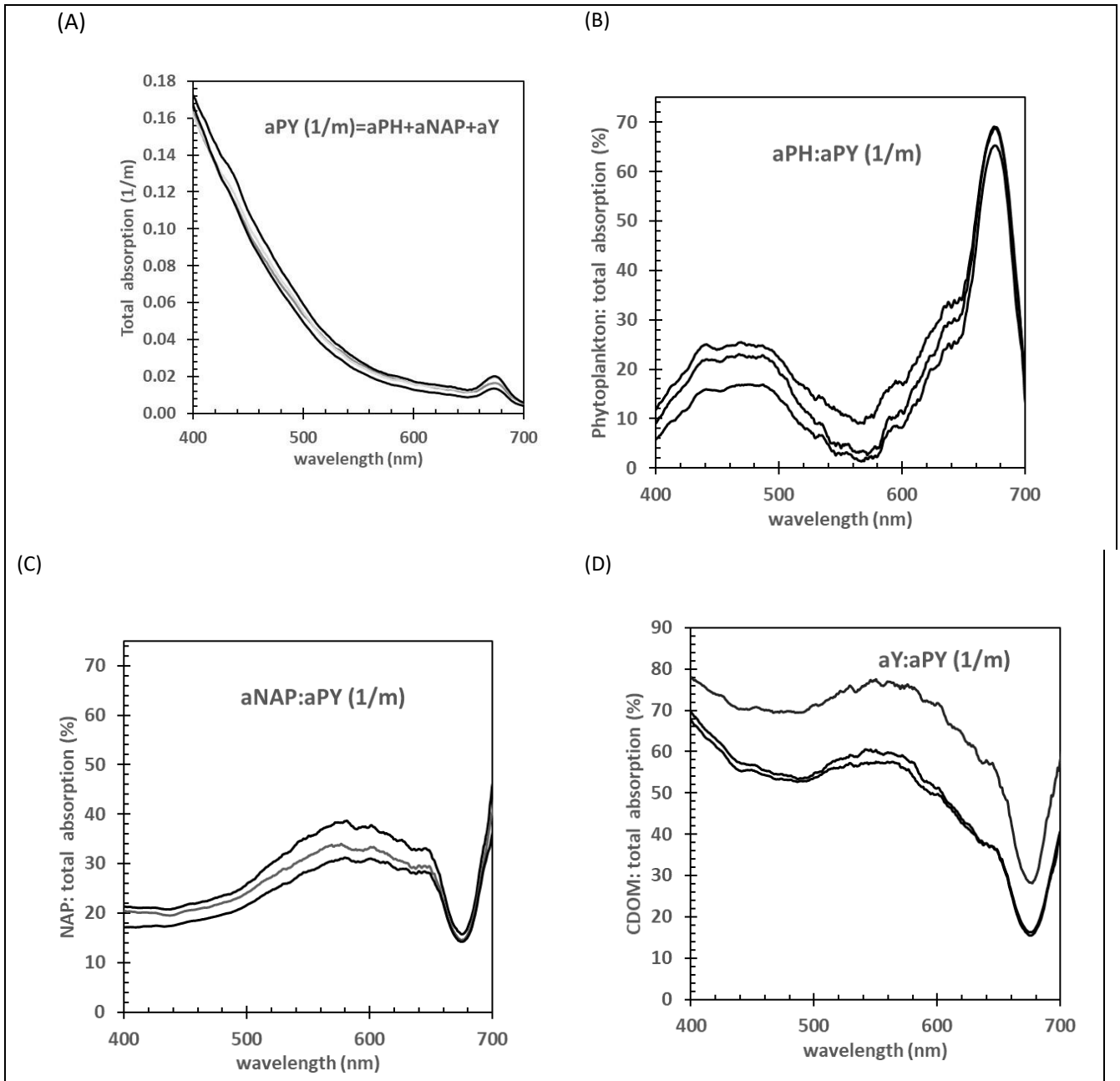

FIGURE 11 ABSORPTION BUDGETS. (A) TOTAL ABSORPTION IS THE SUM OF PHYTOPLANKTON, NAP AND CDOM ABSORPTION, (B) PHYTOPLANKTON ABSORPTION CONTRIBUTION TO TOTAL ABSORPTION, (C) NAP ABSORPTION CONTRIBUTION TO TOTAL ABSORPTION AND (D) CDOM ABSORPTION CONTRIBUTION TO TOTAL ABSORPTION.

Mass specific light absorption properties, also referred to as specific inherent optical properties (SIOPs), represent the efficiency with which a substance or material absorbs light per unit mass. They serve as a quantitative measure of the light absorption capability relative to the mass of the substance. These properties are particularly valuable in environmental and biological studies, as they help elucidate the light absorption characteristics of various components present in aquatic ecosystems, such as phytoplankton, nonalgal particles, and dissolved organic matter. By examining mass specific light absorption properties, researchers can gain insights into the effectiveness and contribution of these components to the overall light absorption within a given system.

In the case of Boston Bay (Figure 12), it has been observed that mass specific CDOM (Coloured Dissolved Organic Matter) absorption is relatively higher than TSS specific aP (a*P) in the blue region of the spectrum. However, in the green and red regions, its efficiency tends to be lower than that of particulate matter. Across multiple samples, the coefficient of variance for a*P showed spectral variations between 10% and 25%. On the other hand, a*PH exhibited a wide range of variations, spanning from 5% to 75%, with a significant shift in the green region. These observed spectral variations in mass specific absorption properties within Boston Bay emphasize the importance of characterizing the bio-optical properties specific to the region and developing a spectral library tailored to that domain. Such efforts would facilitate the implementation of domain-specific remote sensing models and improve the accuracy of retrieving water quality parameters.

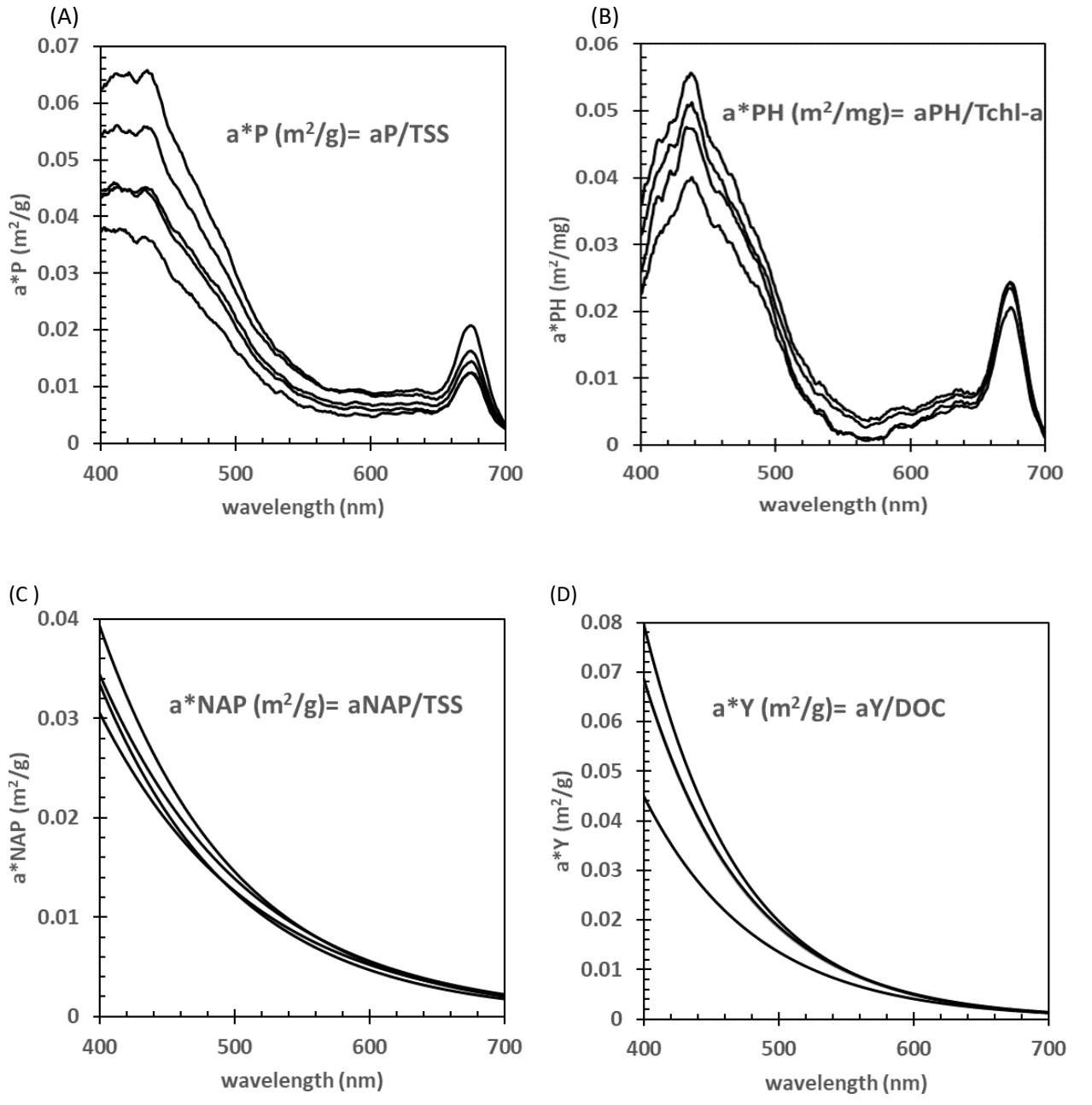

FIGURE 12 MASS SPECIFIC ABSORPTION PROPERTIES. (A) TSS SPECIFIC PARTICULATE ABSORPTION, (B) TCHL-A SPECIFIC PHYTOPLANKTON ABSORPTION, (C) TSS SPECIFIC NAP ABSORPTION AND (D) DOC SPECIFIC CDOM ABSORPTION.

5 Empirical Algorithm Development and Evaluation

Empirical algorithms have been used extensively throughout the aquatic remote sensing literature (Table 3). These algorithms can provide a simple method for retrieving water quality information based on limited spectral information. In this project an empirical approach was adopted as a method to demonstrate the potential to integrate *in situ* radiometric and water quality measurements with remote sensing data. Figure 13shows the algorithm development process adopted for this project, in this process in-water sensor data and radiometric data from the HydraSpectra undergo a calibration and quality assurance process (see section 4). Additionally, the radiometric data undergoes a convolution process to transform it from hyperspectral data with a spectral resolution of 1 nm to the spectral bands of the intended remote sensing sensor (LS8/9). Once the radiometric data has the same spectral resolution as the LS8/9 it is merged with the in-water sensor data and simultaneous acquisitions are used to build empirical relationships between spectral features and water quality parameters. Once established, these relationships are then applied to the remote sensing data to derive water quality maps of the Spencer Gulf region. This section describes the fulfillment of deliverable D4.

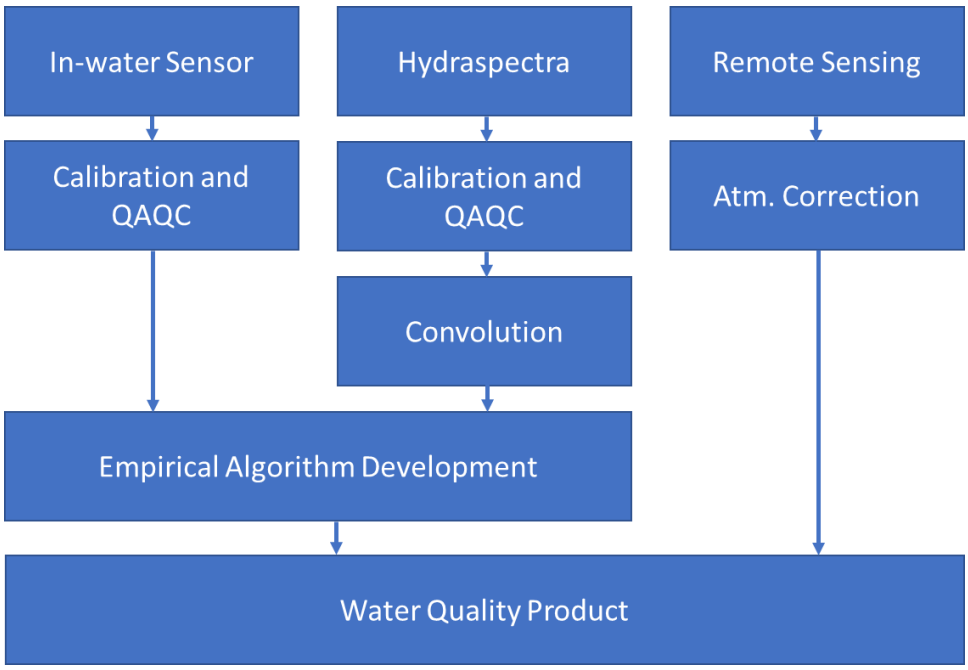

FIGURE 13 EMPIRICAL ALGORITHM DEVELOPMENT PROCESS

5.1 Data Integration

5.1.1 HydraSpectra Data

HydraSpectra data were acquired through the ADIAS platform using the integrated database that acquires the data from the Senapse platform (https://products.csiro.au/senaps/). A total of 10,855 measurements were available for this project. Figure 14shows the density of HydraSpectra

measurements prior to the application of quality control procedures. The data show that they HydraSpectra is largely returning spectra with a shape typical of blue oceanic waters.

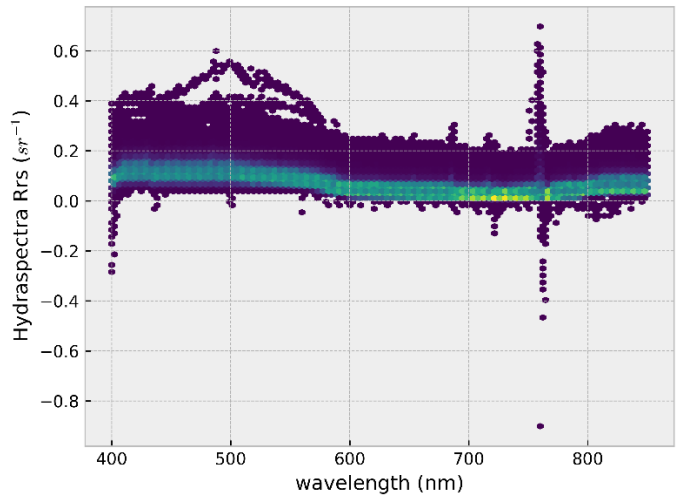

FIGURE 14: DENSITY IF HYDRASPECTRA MEASUREMENTS PRIOR TO APPLICATION OF QAQC

Prior to QAQC the HydraSpectra was returning a maximum of 42 observations per day (Figure 15). Some irregularity in observation frequency is observed throughout the study period with missing observations appearing more frequently in the period from February 2022 until March 2023.

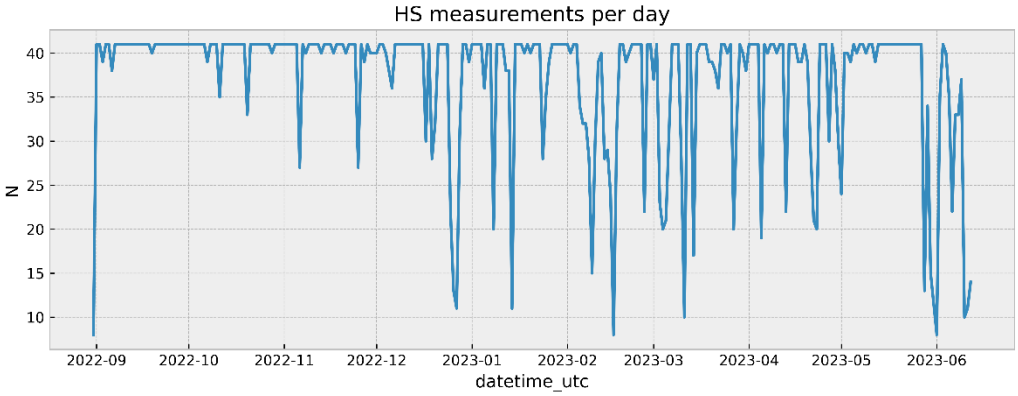

FIGURE 15: HYDRASPECTRA MEASUREMENT FREQUENCY PRIOR TO QAQC

It is well known that the quality of radiometric measurements are influenced by low sun angles that occur early and late in the day. To improve the expected quality of HydraSpectra measurements, only observations that occurred between 11:30 and 13:30 were retained for further use in this study. Other factors that may influence the quality of HydraSpectra data include tilt angle, solar azimuth and substances such as sea-spray occluding the sensor windows. Following time filtering a maximum of 9 observations per day were available (Figure 16).

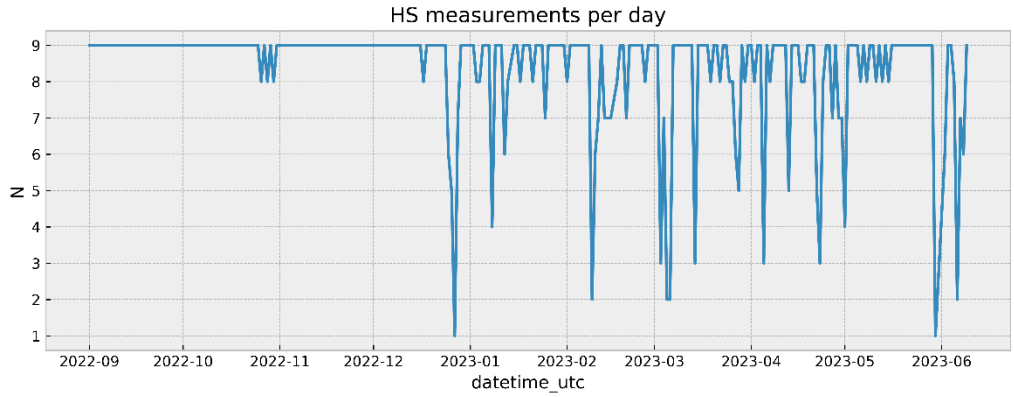

FIGURE 16: HYDRASPECTRA MEASUREMENT FREQUENCY FOLLOWING QAQC

5.1.2 In-water Sensor Data

In water parameters were measured by a YSI EXO multiparameter sonde (see section 4.2). The measurements relevant to this study include indicators of chlorophyll-a (CHL-a) concentration, turbidity and the concentration of coloured-dissolved organic matter (CDOM). Both CHL-a and CDOM were measured by fluorescence sensors, CHL-a fluorescence was subsequently converted to physical units of µg/L by calibration coefficients determined by the manufacturer during calibration. CDOM concentration is expressed in quinine sulphate units (QSU). As CDOM was determined by fluorescence it will be referred to as fDOM.

Chlorophyll-a

CHL-a concentrations over the study period are shown in Figure 17. During servicing grab samples were collected and analysed by HPLC to provide an independent check on sensor readings. The CHL-a concentrations determined by the two methods match fairly well, however some dispersal of HPLC samples can be seen for the February 2023 servicing trip.

CHL-a data from the in-water sensors was smoothed using a moving average of 20 measurements. The smoothed data are shown in Figure 17.

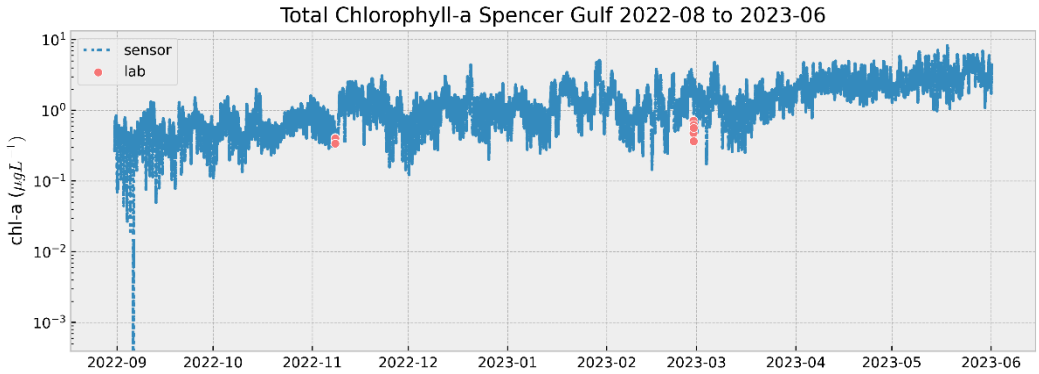

FIGURE 17 CHLOROPHYLL-A CONCENTRATION AT THE SPENCER GULF BUOY 2022-08-01 TO 2023-06-01. HPLC ANALYSIS FROM GRAB SAMPLES COLLECTED ON TWO SERVICING TRIPS ARE SHOWN AS RED CIRCLES.

Turbidity

The turbidity sensor exhibited significantly more noise, temporal discontinuities and drift. During the maintenance trip in water sensors are exchanged with freshly calibrated sensors, which was likely the cause of the step changes observed. The magnitude of these step changes is small and are likely evident only due to the low turbidity at the site. To correct for these effects smoothing, linear drift correction and an offset correction were applied to ensure a stable dataset (Figure 18).

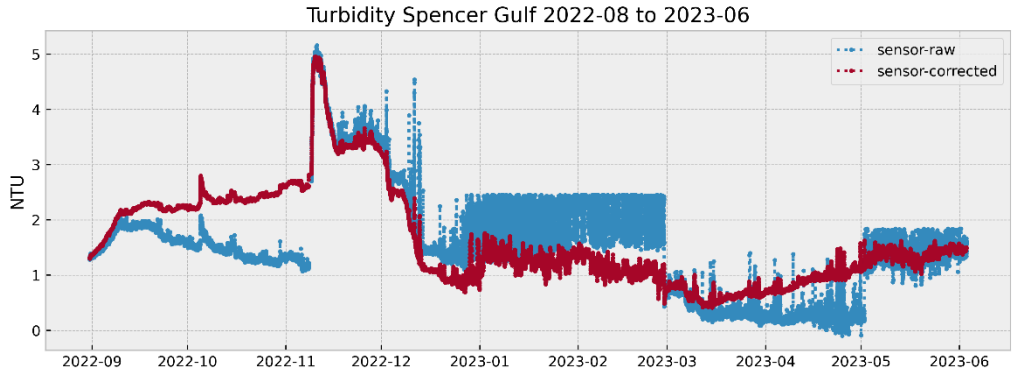

FIGURE 18 RAW AND SMOOTHED TURBIDITY FROM THE IN-WATER SENSOR

Very little range in turbidity was observed during the study period (Figure 19). This low dynamic range accentuated the small step changes that were observed after the sensors were exchanged during the servicing trips. While discontinuities are observed they amount to 1-2 NTU which represents only minor change in optical properties. The low dynamic range observed by the in-water sensors are unlikely to significantly influence the optical properties of the water.

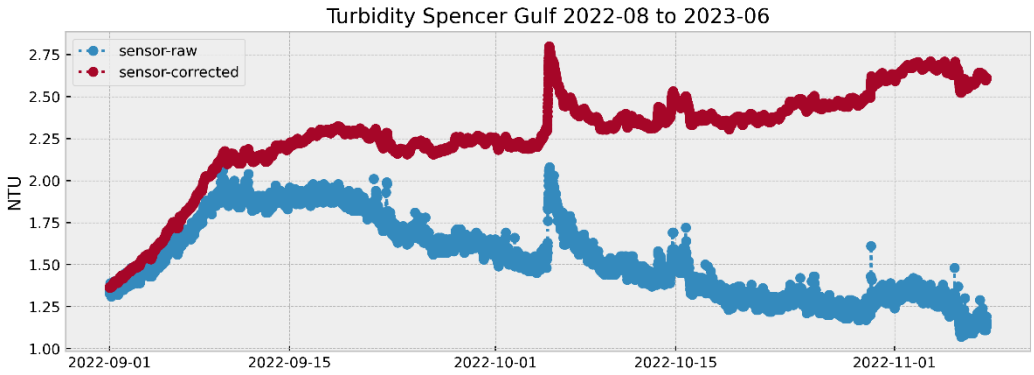

FIGURE 19 INSERT OF FIGURE 18 SHOWING THE EXTENT TO WHICH TURBIDITY DATA WAS REQUIRED TO BE CORRECTED.

fDOM

The raw and corrected data for fDOM are shown in Figure 20. During the observation period, very little variation in fDOM was observed. The levels of fDOM were insignificant enough that the in-water sensor showed a significant negative bias. The dynamic range of fDOM observed is unlikely to result in an observable change in radiometric characteristics of the water, and as a result is not expected to be observable by the empirical algorithms.

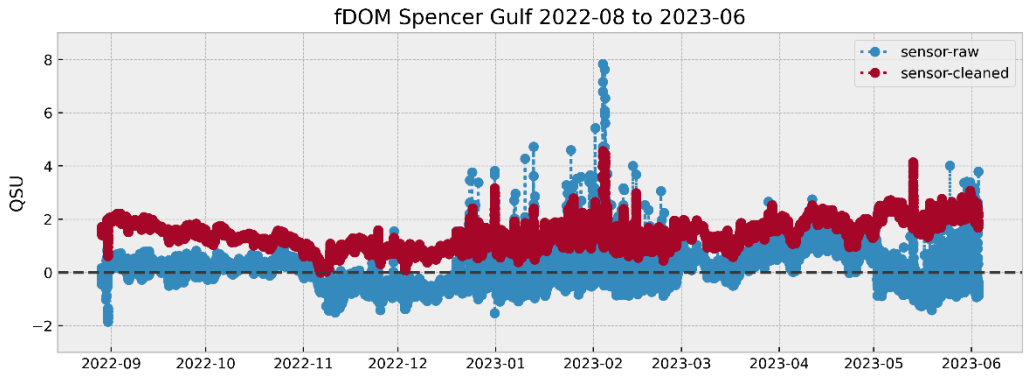

FIGURE 20 RAW AND CLEANED FDOM FROM IN-WEATER SENSORS.

5.1.3 Remote Sensing Data

The Landsat mission provides a comprehensive global dataset of observations dating back to the 1980's. Level 1 top-of-atmosphere data from the Landsat 8 and Landsat 9 (LS8/9) missions were acquired and atmospherically corrected using the ACOLITE (Vanhellemont and Ruddick (2018)) processing system. ACOLITE was reconfigured to substantially improve processing efficiency to facilitate implementation of the full LS8/9 archive. The atmospherically corrected data was retained and indexed into ADIAS's database. These datasets provided 170 LS8 observations and 28 LS9 observations between January 2014 and March 2023. Figure 21 shows the Landsat tiles ingested into the ADIAS database, while Table 2 provides a description of the band names and abbreviations used in the text.

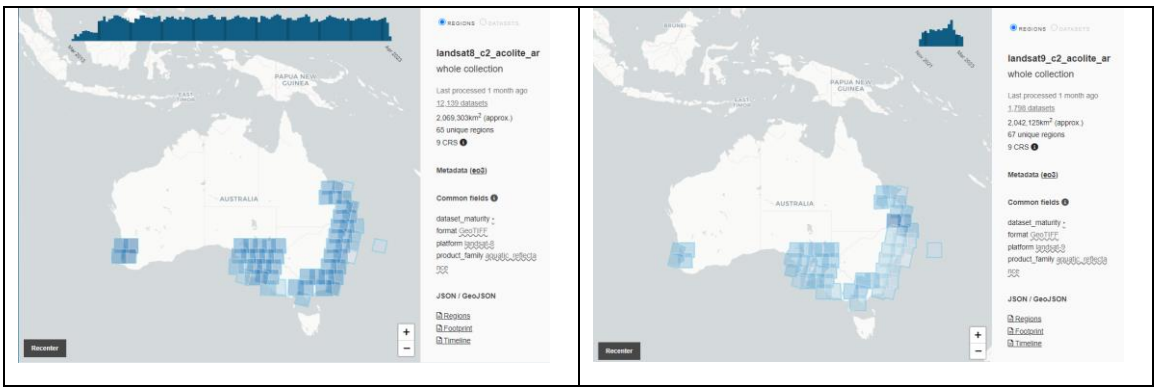

FIGURE 21 ATMOSPHERICALLY CORRECTED LANDSAT8/9 DATASETS HOUSED ON THE ADIAS PLATOFRM

The Sentinel-2 mission uses a pair of satellites (S2A and S2B) to obtain data at 10m spatial resolution and 5-day temporal resolution. These data have been used extensively for water quality observations in lakes and reservoirs. However, these data were not used as part of this project as visible striping was observed for data in the coastal areas Figure 22. Striping such as this is known to occur because of subtle differences in satellite optics which become apparent in regions of low signal strength such as Spencer Gulf. As the striping would have introduced artefacts into this analysis, Sentinel-2 data was not used for this project.

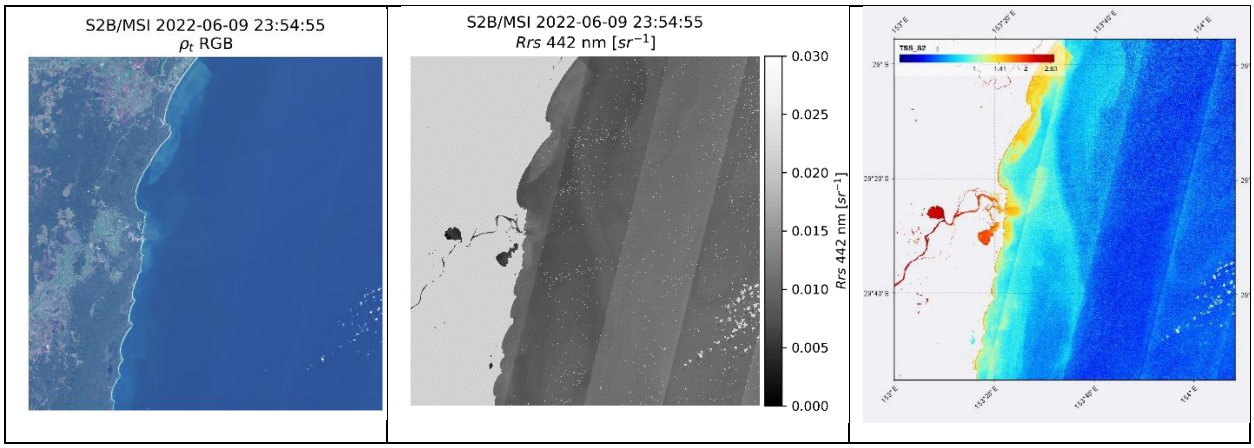

FIGURE 22 EXAMPLE IMAGE OF STRIPING IN SENTINEL 2B (2022-06-09) SHOWING AUSTRALIAN COASTAL WATERS (NSW). THE LEFT PANEL SHOWS A TRUE COLOUR IMAGE, CENTRE SHOWS 442 NM BAND AND RIGHT PANEL SHOWS OUTPUT OF A EMPIRICAL ESTIMATE OF TSS.

A kernel of 3x3 pixels was selected centred on the geographical coordinates of the Spencer Gulf buoy, and data extracted for each band over the full time series. For further analysis the kernel mean was used for each Landsat band and is shown in Figure 23. The performance of the atmospheric correction was qualitatively assessed by observing the magnitude of remote sensing reflectance (Rrs) at the NIR band. Low turbidity waters exhibit very low Rrs in this band due to strong absorption of water. While this is typically observed for this dataset, some observations show extremely high Rrs at NIR indicating possibly poor performing atmospheric correction. All observations conform to the expected spectral shape of blue oceanic waters with low dissolved solids, chlorophyll and CDOM concentrations.

TABLE 2 LANDSAT8/9 BAND NAMES AND ABBREVIATIONS USED IN THE TEXT.

Band Name	Abbreviation	Band Width (nm)	
		LS8	LS9
Coastal Aerosol	V	430-450	430-450
Blue	B	450-451	450-510
Green	G	530-590	530-590
Red	R	640-670	640-670
Near-infrared	NIR	850-880	850-880

This above section describes the acquisition of historical and new satellite data to satisfy requirements in deliverable D4.

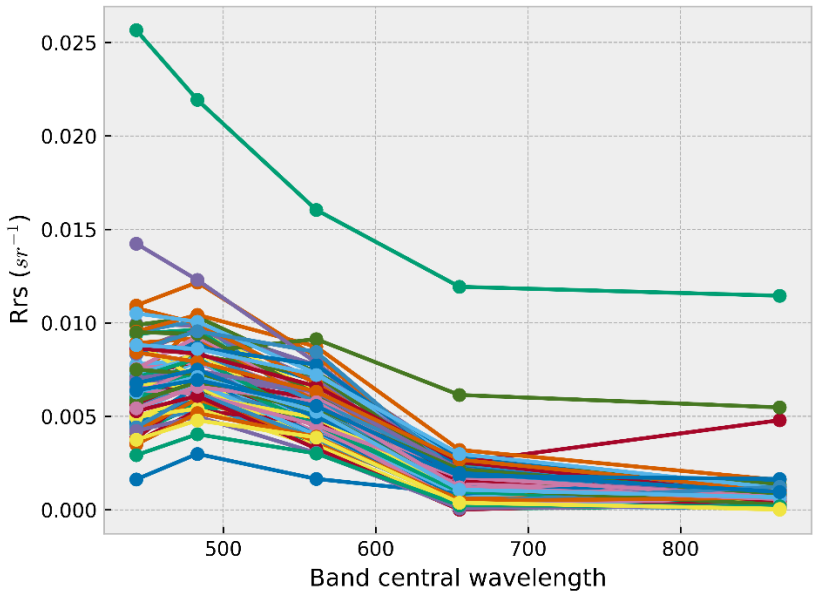

FIGURE 23: MEAN OF 3X3 PIXEL GRID CENTRED ON LOCATION OF BUOY

5.1.4 Comparison of HydraSpectra and match LS8/9 data

This section describe test and validation activities conducted to satisfy part of deliverable D4 and D5.

The algorithm development strategy adopted for this project aims to use paired in-water and radiometric measurements from *in situ* instruments and apply the observed relationships to remote sensing data. Discrepancies between *in situ* and remotely sensed radiometric measurements are likely to result in errors in predictions of in-water quantities using the remotely sensed data. Thus, it is important to acquire fiducial reference radiometric measurements to provide a comparative baseline with which to compare the HydraSpectra and remote sensing data. However, it was not possible to collect such data for this project and, consequently, only a qualitative comparative analysis can be made here.

Landsat-8/9 data described in section 5.1.3 were paired with HydraSpectra measurements obtained within a 15-minute window of the satellite overpass. As Landsat observations occur earlier than the time window used for HydraSpectra quality control, non-QAQC HydraSpectra data were required to be used for this comparison. Only quality controlled HydraSpectra data was used in subsequent analysis.

Only nine coincident HydraSpectra and Landsat observations were able to be acquired under clear sky conditions during the study period. Despite the limited number of observations, it can be seen in Figure 24 both the HydraSpectra and Landsat spectral shapes are typical for blue oceanic waters as expected given the in-water observations. Despite this, for most bands the HydraSpectra data is approximately 20 times higher than the Landsat observations (Figure 24). At present, HydraSpectra postprocessing does not account for the presence of neutral density filters protecting the radiance and irradiance sensors. Work is ongoing to include corrections for the spectral sensitivity of these filters, which is expected to reduce the high R_{rs} values observed here. A comparison of HydraSpectra and Landsat observations bands is shown in the lower four panels of Figure 24. These comparisons do not show a linear relationship between HydraSpectra and Landsat. It is expected that this lack of linearity is the result of errors in both the HydraSpectra and the Landsat observations as well as the lack of spectral variability observed in Boston Bay across the measurement period. The collection of radiometric fiducial reference

measurements, and/or the careful collection of grey panel reference measurements of the HydraSpectra would be required to determine the magnitude of error from each source.

Furthermore, a positive linear relationship is not observed when comparing the bands directly (see lower four panels of Figure 24).

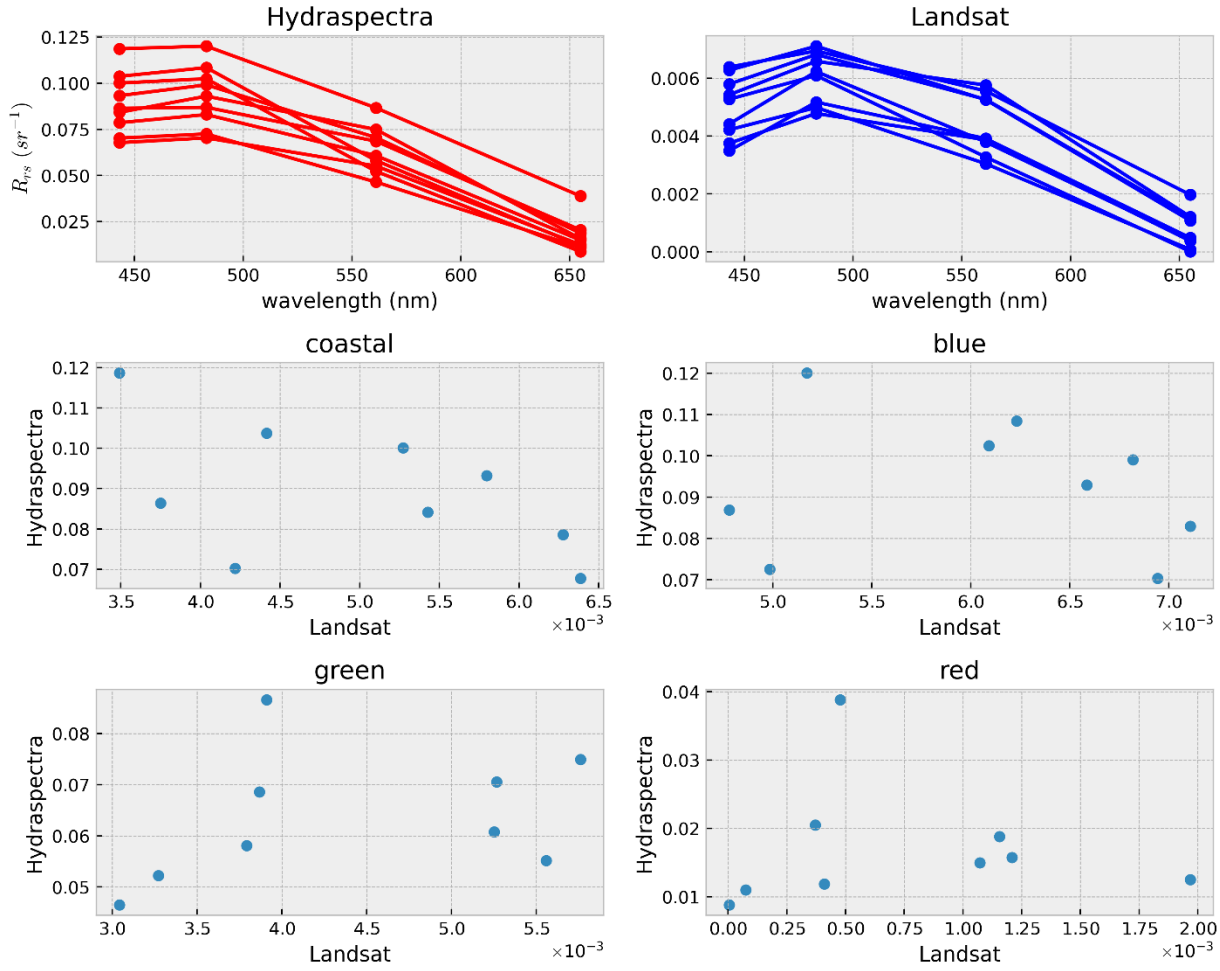

FIGURE 24 COINCIDENT HYDRASPECTRA AND LANDSAT OBSERVATIONS

Most of the empirical algorithms evaluated for this study employ band ratios to encode information about spectral shape. To examine potential sensitivity of algorithms to differences in the relative magnitude of bands, all combinations of band ratios in the visible range were plotted for the coincident HydraSpectra and Landsat data (Figure 25). The only combination of bands which conform to a linear relationship are the coastal/green and blue/green pairs. Previous studies evaluating atmospheric correction typically show that the green bands are best retrieved, while bands <480 nm show the worst performance.

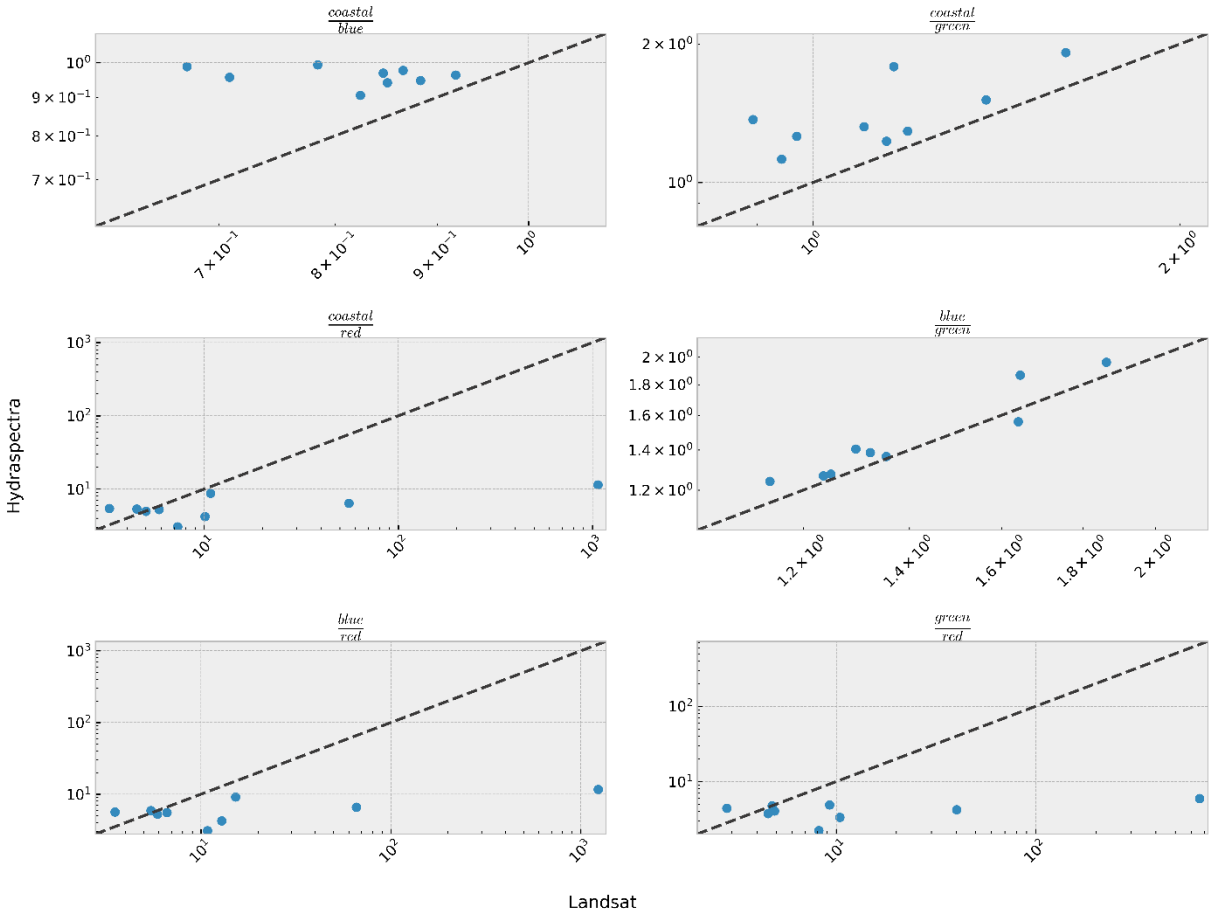

FIGURE 25 BAND RATIOS FOR COINCIDENT HYDRASPECTRA AND LANDSAT OBSERVATIONS. A COMPARISON IS SHOWN BETWEEN LANDSAT (X-AXIS) AND HYDRASPECTRA (Y-AXIS) FOR ALL COMBINATIONS OF BAND RATIOS IN VISIBLE RANGE.

5.1.5 Integration of *in situ* radiometric and in-water data

This section described data integration activities undertaken to satisfy deliverable D4.

The *in situ* in water and radiometric datasets were merged by selecting measurements that occurred within two minutes of each other. This resulted in 1251, 1051 and 1260 HydraSpectra measurements paired with CHL-a, turbidity, and fDOM measurements, respectively. A basic analysis was then undertaken to observe the extent to which ratios between the blue, green and red bands correlated with the in-water parameters.

As can be seen in Figure 26 only the blue/green ratio shows a strong relationship to the concentration of CHL-a. This relationship was robust for both the corrected (smoothed) and raw datasets.

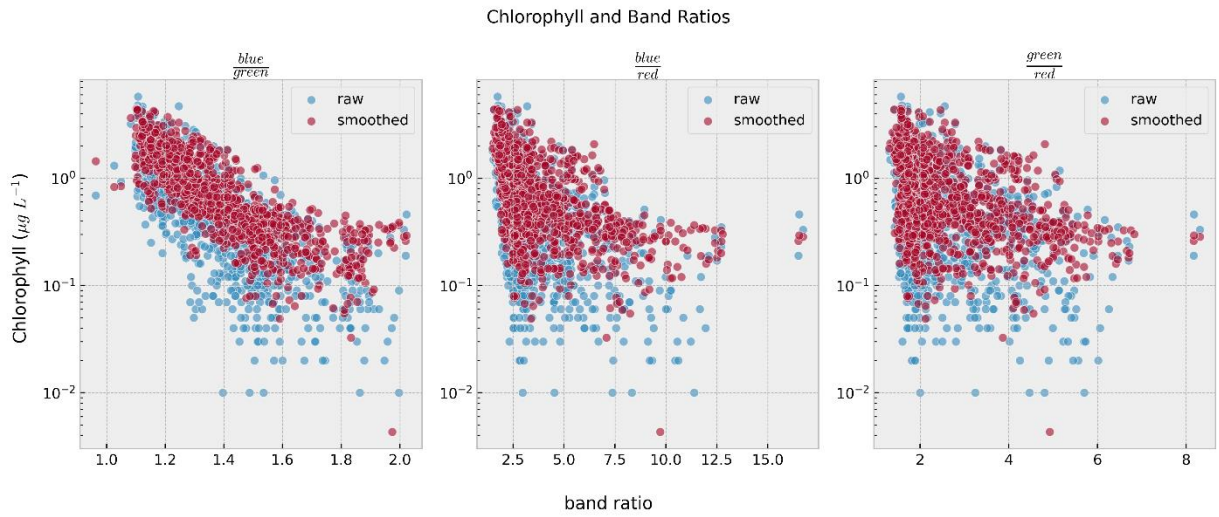

FIGURE 26 CORRELATION OF CHL-A MEASUREMENTS WITH RATIOS OF THE BLUE, GREEN AND RED BANDS. NOTE CHL-A IS SHOWN ON A LOG-SCALE. FOR COMPARISON RAW DATA IS ALSO PLOTTED.

Turbidity showed no relationship to any band ratio (Figure 27). It is expected that the low dynamic range of the turbidity dataset influenced this result. Turbidity ranges from 0-5 NTU is not expected to strongly influence the optical properties of the water.

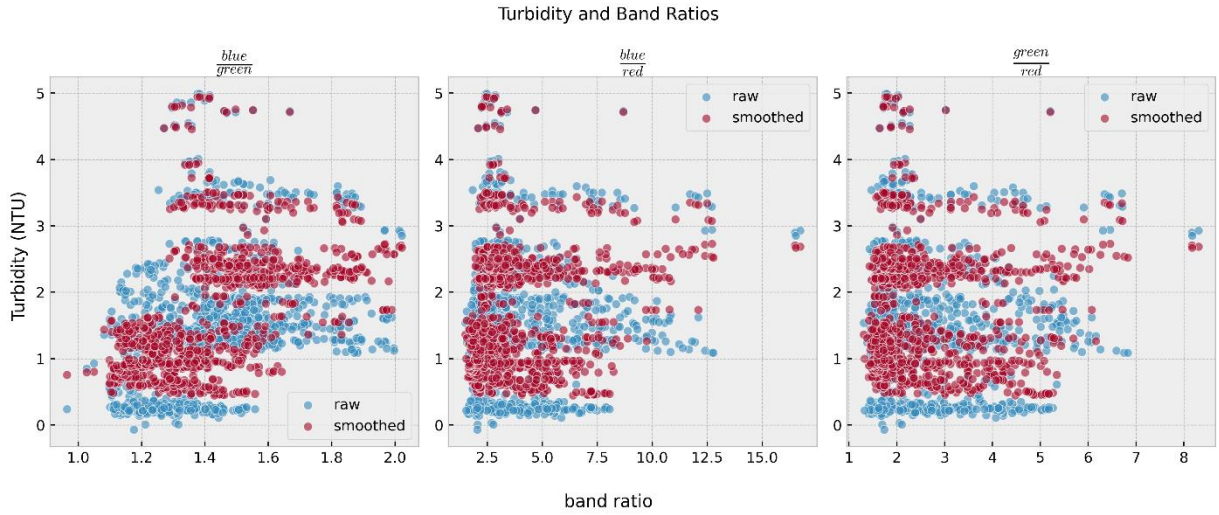

FIGURE 27 CORRELATION OF TURBIDITY MEASUREMENTS WITH RATIOS OF THE BLUE, GREEN AND RED BANDS. SHOWING BOTH THE CORRECTED (SMOOTHED) DATA AND THE RAW DATA.

Similarly, , fDOM exhibited a very low dynamic range in this study and as a result correlated poorly with all band ratios (Figure 28).

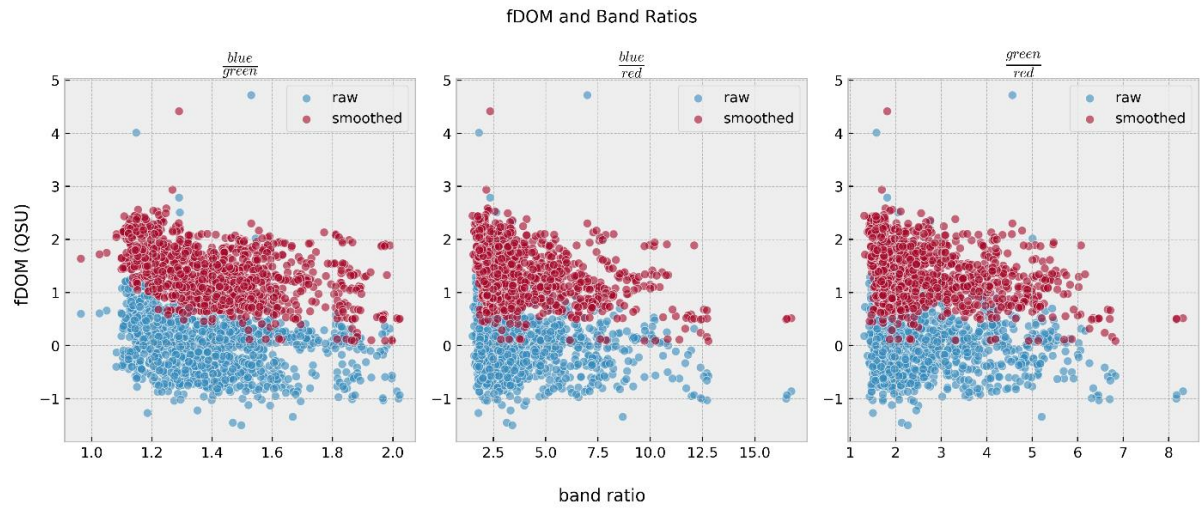

FIGURE 28 CORRELATION OF FDOM MEASUREMENTS WITH RATIOS OF THE BLUE, GREEN AND RED BANDS. SHOWING BOTH THE CORRECTED (SMOOTHED) AND RAW DATA.

5.1.6 Empirical algorithms

This section describes the implementation and evaluation of water quality indices undertaken to satisfy deliverable D4.

An extensive array of empirical algorithms designed to retrieve water quality parameters from multi-spectral and hyper spectral satellites are available in the literature. A range of empirical algorithms suitable for use on Landsat 8 data were selected for evaluation. Table 3 describes the algorithms selected for use in this study. Algorithms were selected on the basis of being applicable to Landsat imagery, and by their evaluation in the original paper. Algorithms from coastal, oceanic and inland waters have been included.

As the parameters of empirical algorithms tend to vary by location and water type, the parameters of each algorithm were obtained by fitting the empirical algorithms to all available time-matched HydraSpectra and in-water quality variables. Algorithm performance was then evaluated using mean absolute error (MAE) and bias (Equation 1, Equation 2) after Seegers et al. (2018). In the form provided here, MAE will always be >1, and represent the percentage relative error, such that a MAE of 1.5 indicates a relative error of 50%. The bias metric indicates the sign of the relative prediction error, with 1.2 indicating a relative over prediction of 20%, and 0.8 an underprediction of the same magnitude. As both performance metrics are evaluated in log space, any negative prediction was removed from analysis prior to evaluating the performance metrics.

TABLE 3: EMPIRICAL ALGORITHMS SELECTED FOR USE IN THIS STUDY. THE VARIABLES V,B,G,R DESIGNATE THE COASTAL AEROSOL, BLUE, GREEN AND RED BANDS RESPECTIVELY. ALGORITHM PARAMETERS ARE DESIGNATED $P_I..P_N$.

Name	Algorithm	Reference
TSS1	$TSS = p_1 \times \exp(p_2) \times \left(\frac{g+r}{2}\right)$	Dekker et al. (2002)
TSS2	$TSS = p_1 \times \left(\frac{b}{r}\right)^{p_2}$	Woźniak (2014)
TSS3	$TSS = p_1 - p_2 \times \left(\frac{r}{g}\right)$	Wang et al. (2006a)
CDOM1	$CDOM = p_1 \times \left(\frac{g}{b}\right) - p_2$	Koponen et al. (2007)
CDOM 2	$CDOM = p_1 \times \left(\frac{r}{g}\right)^{p_2}$	Kutser et al. (2005)
CDOM3	$CDOM = 10^{(p_0+(P_1\times x)+(p_2\times x^2))}$ $where, x = log_{10}\left(\frac{b}{g}\right)$	Kowalczuk et al. (2005)
CHL1	$CHL = p_1 \times \left(\frac{b-r}{g}\right)^{p_2}$	Mayo et al. (1995)
CHL2	$CHL = 10^{y}$ $where, y = P_1 + p_2 \times \log\_10(v) + (p_3 \times x)$ $where, x = \frac{v}{r}$	Han & Jordan (2007)
CHL3	$CHL = exp\left(p_1 + P_2 \times r + \left(p_3 \times \frac{b}{r}\right)\right)$	Brezonik et al. (2005)
CHL4	$CHL = p_1 - p_2 \times (b-g)$	Wang et al. (2006b)
CHL5	$\log_{10} CHL = p_0 + (p_1 \times X) + (p_2 \times X^2) + (p_3 \times X^3) + (p_4 \times X^4)$ $where, X = \log_{10}\frac{b}{g}$	Werdell et al. (2018)

$MAE = 10^{\wedge}\left(\sum_{i=1}^{n} \frac{\lvert\log_{10} M_i - \log_{10} O_i\rvert}{n}\right)$	Equation 1

$bias = 10^{\wedge}\left(\sum_{i=1}^{n} \frac{\log_{10} M_i - \log_{10} O_i}{n}\right)$	Equation 2

5.1.7 Algorithm performance evaluation

Algorithm performance was strongly related to the observed dynamic range of the water quality parameter. In the case of CDOM and TSS/turbidity where the dynamic range of the parameter was not expected to strongly influence Rrs, relatively poor performance was observed.

Algorithm performance is shown in Figure 29. Algorithms based on polynomial sequences (CDOM3 and CHL5) showed the best performance with neutral bias and the lowest MAE. The TSS/turbidity algorithms showed the poorest performance with high MAE, and many returned negative turbidity values.

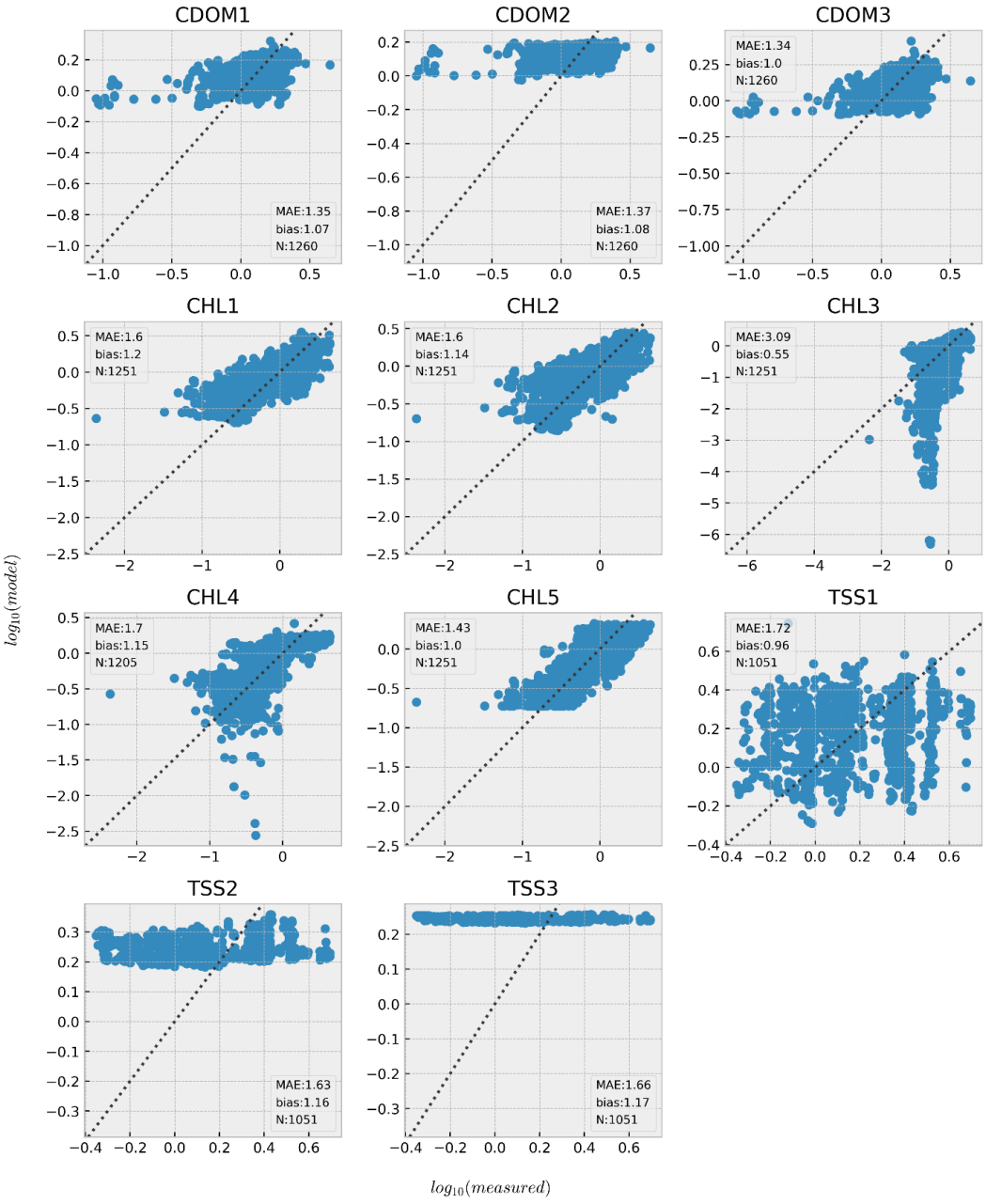

FIGURE 29 PERFORMANCE OF EMPIRICAL ALGORITHMS USING ALL AVAILABLE MATCHED HYDRASPECTRA AND IN-WATER BUOY DATA. THE NUMBER OF GREATER THAN 0 IS GIVEN AS N. NOTE BOTH AXES ARE PLOTTED AS LOG_{10}.

CHL5 was the best performing algorithm. This algorithm is based on NASA's global chlorophyll-a product for Landsat sensors known as OC3. This algorithm uses a 4^{th}-order polynomial to retrieve chlorophyll concentration. The parameters for this algorithm are tuned from a dataset spanning four orders of

magnitude. As the in-water observations used in this case span 0-4 µg L^{-1} it is expected that the algorithm parameters presented here are overfit to relatively low CHL concentrations, and as a result are not expected to generalise well.

A visual inspection of timeseries data was also conducted. Figure 30 shows representation of CHL, fDOM and turbidity from the in-water sensors (measured), and the best performing empirical algorithm applied to the HydraSpectra (model) and Landsat-8/9. For CHL good concordance from all methods is seen between 0.5 and 2 µg L^{-1}. However, as measurements increase above 2 µg L^{-1} the in-water measurements diverge from the HydraSpectra (no Landsat data was available for this period). Future analysis is required to establish the effect that in-water quality assurance corrections have on the accuracy of empirical algorithms.

(A)

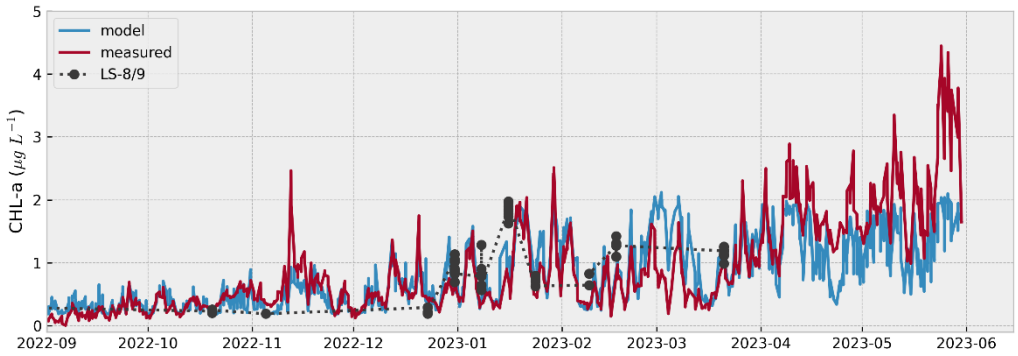

(B)

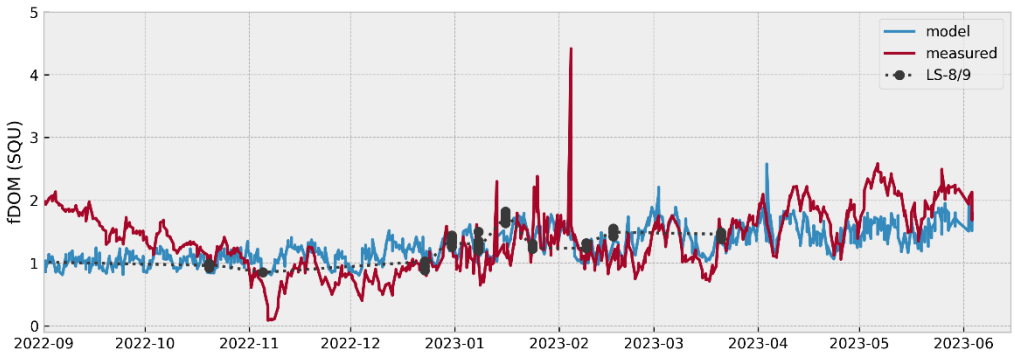

(C)

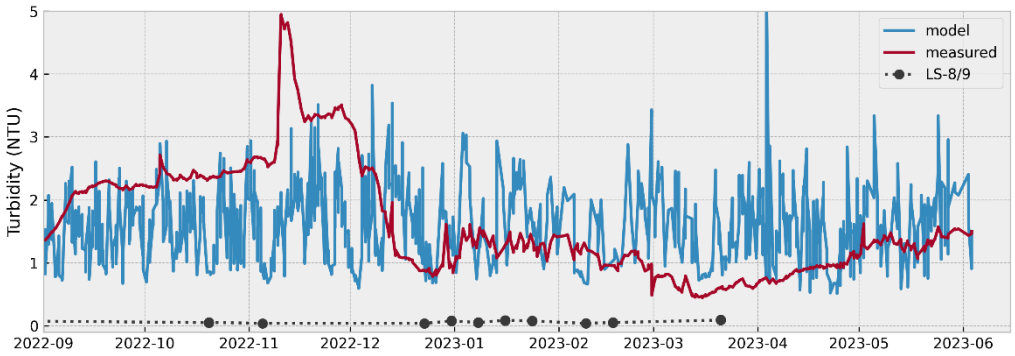

FIGURE 30 TIMSERIES SHOWING IN-WATER MEASUREMENTS (MEASURED) OVERLAYED WITH THE BEST PERFORMING EMPIRICAL MODELS APPLIED TO THE HYDRASPECTRA (MODEL) AND LANDSAT (LS-8/9) DATA. (A) SHOWS CHL-A USING CHL5, (B) FDOM USING CDOM3, AND (C) TURBIDITY USING TSS1.

fDOM is well predicted, though this may be expected given the dynamic range is very small. The CDOM3 model underpredicts fDOM in the early part of the study period and shifts to overpredict in the later part of the study period. As with CHL5, further evaluation is required to understand the sensitivities of QAQC procedure on algorithm accuracy.

Turbidity is poorly predicted by all the TSS models. From Figure 30(C) the TSS1 model applied to the HydraSpectra varies around a mean prediction of 1.5 NTU and is insensitive to changes in measured NTU. Further it can be seen that there is a lack of agreement between TSS1 applied to the HydraSpectra and Landsat data. Unlike CHL5 and CDOM3, which exclusively use band ratios, TSS1 uses the absolute value of the green and red bands in its calculation (see Table 3). It is expected that the large difference between turbidity estimated using Landsat and HydraSpectra data is due to the weak correlation between HydraSpectra and Landsat bands shown in Figure 25 and the poor correlations between HydraSpectra band ratios and turbidity shown in Figure 29. As part of other AquaWatch work-packages work is ongoing to identify the source of these offsets and implement solutions. Future work would benefit from obtaining radiometric fiducial measurements matched to HydraSpectra and Landsat observations to provide independent validation of these data. This will be especially relevant to work that seeks to evaluate the efficacy of various atmospheric correction algorithms for the Spencer Gulf region.

To examine sensitivities in the application of empirical algorithms in this region, a timeseries analysis of the CHL5 algorithm was undertaken. CHL5 was applied to the full Landsat8 archive (2014-2023), the mean and coefficient of variance were calculated. Additionally, at four locations CHL5 was applied to the full time series, and probability density plots rendered to examine the behaviour of the algorithm.

Within Boston Bay, CHL5 produced mean CHL-a results within the range measured by the in-water sensors (Figure 31(A)). This implies that the model was able to capture the CHl-a ranges that it was exposed to within a localised area. Significant variation in mean CHL-a was observed throughout Spencer Gulf (Figure 31(B)). Unrealistically high mean CHL-a was observed in the central region of the Gulf, propagating out to the open ocean, these regions also exhibit the greatest variability in CHL-a as indicated by the coefficient of variance. Figure 31(C) shows that the distribution of CHL-a contains a relatively small number of very high values at Corny Point, and plurality of unrealistically high estimations at the Open Ocean site. While the final cause of these errors is beyond the scope of this study, several possible contributing factors detailed below to guide future work.

Figure 32 shows the sensitivity of CHL5 to a range of blue/green band ratios, with the range of band ratios used to fit the algorithm indicated in grey. As blue/green ratios increase above 2.5, CHL5 returns a steep exponential curve, with small changes in the band ratio resulting in large increases in predicted CHL-a concentrations. The overpredicted regions shown in Figure 31(B) exhibit blue/green ratios more than 5, leading to strong overprediction. Thus, the low dynamic range of data encountered by the buoy in Boston Bay and subsequent overfitting is likely to contribute to poor generalisation of the algorithm.

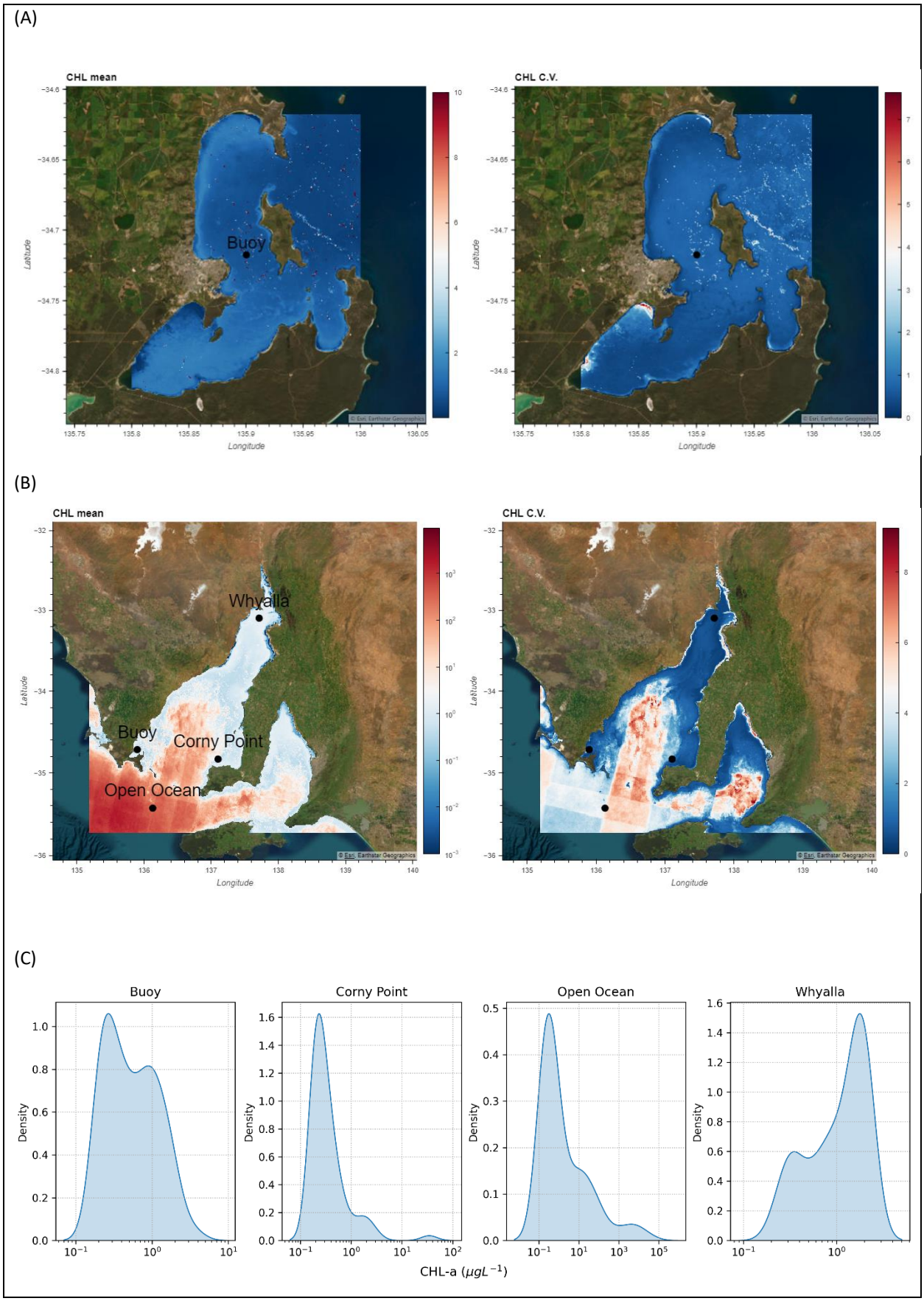

FIGURE 31 LANDSAT 8 (A) MEAN AND COEFFICIENT OF VARIANCE FOR CHL-A DERIVED FROM CHL5 MODEL APPLIED TO LANDSAT TIMESERIES DATA FOR BOSTON BAY (2014-2023), (B)AS EXTRAPOLATED TO THE WHOLE OF SPENCER GULF, AND (C) DENSITY PLOTS OF CHL-A FROM POINTS MARKED ON (A).

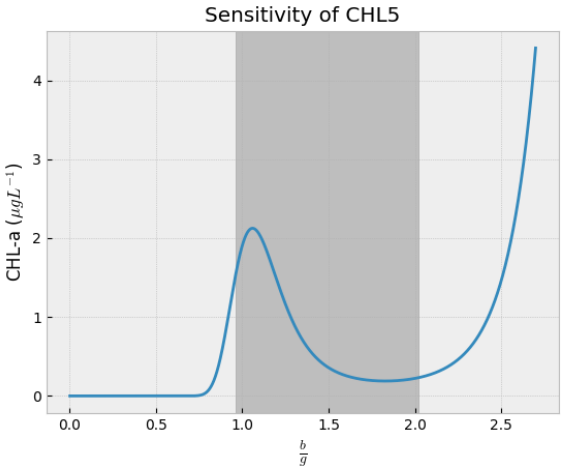

FIGURE 32 SENSITIVITY OF CHL5 TO B/G BAND RATIO, THE RANGE OF B/G RATIO USED IN TRAINING IS SHOWN IN GREY

5.1.8 Data visualisation tools

This section describes activities undertaken to satisfy the development of data visualisation tools to satisfy deliverable D4. Figure 31 is taken from interactive visualisations developed on the ADIAS platform that allow users to investigate the water quality products described in section 5.1.6. These preliminary visualisation tools enable examination of single Landsat observations, or time averaged data and other summary statistics as shown in Figure 31 The visualisation tool also supports obtaining summary visualisations for selected points as shown in Figure 31(C).

6 Summary and Recommendations

6.1 Summary

The Spencer Gulf project has provided a valuable opportunity to integrate diverse data sources that will be relied on for the AquaWatch Mission (project deliverable D6). It provides the first in principle demonstration of water quality observations building on autonomous *in situ* and remote sensing observations as part of the AquaWatch Mission. As such it provides an opportunity for reflection that will assist other pilots and enable them to build on this work. Recommendations and reflections (project deliverables, D6-7) on this project are addressed in the sections below relating to remote sensing data, autonomous *in situ* data collection, storage and processing and independent validation data.

6.1.1 Remote Sensing Data

The ADIAS platform was essential for the acquisition, processing and analysis of all remote sensing data used in this project. ADIAS is in an advanced stage of development and provides essential infrastructure of code and compute that greatly expediate acquisition, storage and analysis of remote sensing data.

The capabilities of ADIAS far outstretched the capacity of other infrastructure to make full and efficient use of those resources. This was most evident in the application of atmospheric correction routines. The ACOLITE code base was developed in Europe to facilitate the retrieval of water quality parameters from a range of satellites. The code was made freely available and is well documented. However, significant modifications were required to efficiently use this code on ADIAS. The significant time investment required to refactor algorithms to efficiently use cloud resources can be a time consuming and highly

specialised skill that has limited availability in AquaWatch. A range of AC and other algorithms will be applied in AquaWatch projects, and it is essential to the success of these projects that resources are not wasted through inefficient implementation.

It is well known that the quality of water quality products from satellite observations are highly sensitive to atmospheric correction (Pahlevan et al. 2021). Obtaining fiducial reference measurements (Ruddick et al. 2019) to validate ACOLITE was not possible (time and resource limitation) as part of this project. As a result, it was difficult to adequately validate the performance of ACOLITE for Spencer Gulf waters. Figure 23 shows several observations that do not conform to the expected shape for Spencer Gulf waters. Non-zero Rrs at the NIR band for clear ocean waters indicates inaccurate atmospheric correction. In conjunction with radiometric fiducial reference measurements, a systematic evaluation of AC processes will be necessary to determine the most effective algorithm to use for other pilot projects. It may be that a regional or application-based approach is the most suitable for AC.

Propagation of radiometric uncertainty from remote sensing data to water-quality products has not been included in this project. However, the quantification of uncertainty will be necessary for future AquaWatch projects.

6.1.2 Autonomous *in situ monitoring system and in situ data*

Through this project, we successfully designed, constructed and commissioned an in-situ monitoring system that integrates multiple sensors and consistently streams data in near real-time. The IoT platform used in this project also maintains a historical record of the system status. A thorough analysis of the sensor data and system status data, including the battery voltage history, cable voltage, and system events log, will enable us to evaluate the current system design and identify areas for further improvement. This will include more efficient power and telemetry management, as well as effective system maintenance planning to minimize system downtime and improve the in-situ data quality. Furthermore, we have the opportunity to integrate additional sensors (such as nutrient sensors) or explore new sensing technologies, generating complementary data streams and facilitating the testing of novel technologies.

Currently, we rely on separate dashboards to monitor real-time data streams from the HydraSpectra sensor and all other integrated sensors. With the complete ingestion of all *in situ* data streams into the ADIAS platform, we are now in a good position to create a comprehensive dashboard that consolidates system operation monitoring into a single interface. This unified dashboard will facilitate the maintenance of the system's optimal performance and providing highly relevant and timely information to users.

One of the primary objectives of the Aquawatch mission is to establish an extensive *in situ* sensor network. Encouragingly, our project partner has expressed keen interest in adopting a similar system in the surrounding areas. The successful delivery of this project has paved the path for duplicating the existing system and deploying it in other strategic and vital locations. Additionally, we can explore the possibility of incorporating data streams from monitoring stations established by potential collaborative partners such as IMOS and SA Waters. This expansion will result in the formation of a comprehensive sensor network, providing enhanced spatial coverage for sustainable management of water resources in South Australia's waters.

During this phase of the project, we developed and implemented a series of data processing methods to enhance the quality of the collected HydraSpectra data and the water quality sensor data. However, as we move forward and expand our in-situ sensor network, the volume of data generated is growing exponentially. Therefore, it is crucial that we make dedicated effort to establish a systematic, streamlined, and automated data processing pipeline to handle this influx of ground in-situ sensor data. This pipeline will enable near real-time quality assurance and quality control (QA/QC) of the in-situ sensor data. This data processing and analysis pipeline is essential and critical for validating the earth observation data, enabling more meaningful and useful data analysis, interpretation, and facilitating the development of future data products.

Throughout the project, the *in situ* monitoring station has accumulated substantial sensor data from the HydraSpectra, Water Quality sensors, HAI sensor, and the weather station. Once all the data has been processed and validated, it is crucial to allocate additional effort towards analysing the data to uncover any noteworthy patterns or trends. This analysis may involve utilizing statistical techniques such as regression analysis, time series analysis, or machine learning algorithms to extract valuable insights.

Further projects can also be developed to demonstrate how data generated by Aquawatch can be transformed into downstream data products that has direct benefit to local aquaculture industry. We are currently collaborating with a company to leverage the in-situ data for the development of oxygen forecast models. The product can then be readily utilized for informed decision-making on effective water quality management for water resource managers and operational guidance for local aquaculture farmers.

6.1.3 Data Integration and Algorithm Development

Analysis of the in-water and HydraSpectra data show that these systems can be used to develop inversion algorithms, which are applicable to location in which the data were collected. In this study, a very low dynamic range of in water parameters were observed. While this enabled robust predictions of CHL-a at the study location, the algorithms generalised poorly. As the buoy was operated for a relatively short period of time, it is possible that future data collection will result in greater generalisability. Future work would benefit from more comprehensive bio-optic measurements over a larger collection of water masses, which would facilitate the development of spectral libraries needed to apply machine learning and semi-analytical algorithms for the retrieval of in-water parameters.

The ADIAS platform was pivotal in providing computational, data-handling and storage requirements for this project. All analysis of *in situ* and remote sensing data was performed on ADIAS, and the single development environment greatly facilitated the traceability and reproducibility of these results.

6.1.4 Independent Validation Datasets

Independent validation of satellite remote sensing products is difficult to achieve due to the expense and difficulty of timing high quality sampling to clear sky satellite observations. For this project *in situ* water samples were collected bi-monthly at the buoy and at two other locations. This data included, CHL-a, TSS and CDOM absorption (see section 4.7). In addition, SARDI provided a further 73 samples

collected between 2016 and 2022. This data included CHL-a and TSS measurements. These data were also not timed to coincide with Landsat overpasses and could not be used for direct validation.

6.2 Recommendations

This project has provided valuable experience in implementing an integrated data system to support environmental monitoring in a complex coastal environment. Throughout the project implementation, several lessons were learned, which have led to the following recommendations for future AquaWatch coastal water quality monitoring projects (project deliverable D7):

In situ sensing:

- It is necessary to include a coastal nutrient sensor on the buoy to improve regional understanding of nutrient distributions in Boston Bay, Spencer Gulf. The current study did not incorporate an in situ nutrient sensor.
- The Hyperspectral HydraSpectra sensor would benefit from further analysis of the impact of sensor tilt on optical measurements.
- Biofouling on instruments presents a significant challenge in this coastal site. Increasing the frequency of maintenance visits would help reduce biofouling build-up and associated instrument noise.
- For this coastal site, it is recommended to conduct more frequent on-board calibration of underwater sensors. Onboard calibration of incoming and outgoing sensors in a controlled tank environment would provide better data correction during instrument swaps.
- In the next phase of this project, testing machine-learning based data processing methods to detect and distinguish electronic noise from environmental variability is recommended.
- Conducting frequent water sampling at the buoy location is highly recommended to improve sensor calibrations.
- Establish or adopt a common controlled vocabulary for all *in situ* measurements to facilitate interoperability between AquaWatch data streams.

Remote sensing:

- Improving the spatial coverage of in situ measurements and their representation in remote sensing models would enhance the performance of regional water quality algorithms.
- It is highly recommended to develop and establish optical spectral libraries specifically for the Spencer Gulf region. These spectral libraries would enable the implementation of advanced semi-analytical and machine learning models for various upcoming and new sensors such as Kanyini, CyanoSat, and NASA PACE. These advanced methods are expected to improve the accuracy of retrievals.
- The presence of stripes in Sentinel-2 images limited the utilization of water quality products from this sensor. Future projects should focus on developing a stripe removal model and acquiring additional high-resolution coverage of Boston Bay.
- Future development of satellite remote sensing processing chains in Spencer Gulf region should implement regional atmospheric correction models and compare bottom-of-atmosphere reflectance products in dedicated field campaigns. Such a implementation and comparison would help understand

Visualization:

- Developing a web-based data visualization platform would be more appealing to end users compared to the current data visualization approach using Jupyter Notebooks.

References

Antoine, D., Guevel, P., Deste, J. F., Becu, G., Louis, F., Scott, A. J., & Bardey, P. (2008). The "BOUSSOLE" buoy—A new transparent-to-swell taut mooring dedicated to marine optics: Design, tests, and performance at sea. Journal of Atmospheric and Oceanic Technology, 25(6), 968-989.

Auricht, H., Mosley, L., Lewis, M., & Clarke, K. (2022). Mapping the long-term influence of river discharge on coastal ocean chlorophyll-a. Remote Sensing in Ecology and Conservation, 8(5), 629-643.

Brezonik, P., Menken, K., & Bauer, M. (2005). Landsat-based remote sensing of lake water quality characteristics, including chlorophyll and coloured dissolved organic matter (CDOM). Lake and Reservoir Management, 21(4), 372-382. https://doi.org/https://doi.org/10.1080/07438140509354442

Bricaud, A., Claustre, H., Ras, J., & Oubelkheir, K. (2004). Natural variability of phytoplanktonic absorption in oceanic waters: Influence of the size structure of algal populations. Journal of Geophysical Research: Oceans, 109(C11).

Brodie, J. E., Lewis, S. E., Collier, C. J., Wooldridge, S., Bainbridge, Z. T., Waterhouse, J., ... & Fabricius, K. (2017). Setting ecologically relevant targets for river pollutant loads to meet marine water quality requirements for the Great Barrier Reef, Australia: A preliminary methodology and analysis. Ocean & Coastal Management, 143, 136-147.

Brown, C. J., Jupiter, S. D., Albert, S., Anthony, K. R., Hamilton, R. J., Fredston-Hermann, A., ... & Klein, C. J. (2019). A guide to modelling priorities for managing land-based impacts on coastal ecosystems. Journal of Applied Ecology, 56(5), 1106-1116.

Clementson, L. A. (2012). The CSIRO method. The Fifth SeaW-iFS HPLC Analysis Round-Robin Experiment (SeaHARRE-5).

Cherukuru, N., Martin, P., Sanwlani, N., Mujahid, A., & Müller, M. (2020). A semi-analytical optical remote sensing model to estimate suspended sediment and dissolved organic carbon in tropical coastal waters influenced by peatland-draining river discharges off Sarawak, Borneo. Remote Sensing, 13(1), 99.

Dekker, A. G., Vos, R., & Peters, S. (2002). Analytical algorithms for lake water TSM estimation for retrospective analyses of TM and SPOT sensor data. International Journal of Remote Sensing, 23(1), 15-35.

Dekker, A. G., Vos, R., & Peters, S. (2002). Analytical algorithms for lake water TSM estimation for retrospective analyses of TM and SPOT sensor data. International Journal of Remote Sensing, 23(1), 15-35.

Dickey, T., Lewis, M., & Chang, G. (2006). Optical oceanography: recent advances and future directions using global remote sensing and in situ observations. Reviews of geophysics, 44(1).

Doubell, M. J., James, C. E., & Middleton, J. F. (2015). Modelling of oceanographic variables for the development of additional finfish aquaculture in Spencer Gulf. Final Report prepared for Clean Seas Tuna Ltd. SARDI Research Report Series-South Australian Research and Development Institute, (830).

Doubell, M. and James, C. (2023). Oceanographic monitoring and far-field modelling to inform desalination in Boston Bay. Report to SA Water. South Australian Research and Development Institute (Aquatic Sciences), Adelaide. SARDI Publication No. F2022/000347-1. SARDI Research Report Series No. 1165. 71pp.

Fernandes, M., Cheshire, A., & Doonan, A. (2006). Sediment geochemistry in lower Spencer Gulf, South Australia: implications for southern bluefin tuna farming. Australian Journal of Earth Sciences, 53(3), 421-432.

Ferrari, G. M. (2000). The relationship between chromophoric dissolved organic matter and dissolved organic carbon in the European Atlantic coastal area and in the West Mediterranean Sea (Gulf of Lions). Marine Chemistry, 70(4), 339-357.

Gaylard, S. (2014). Marine Pollution within Spencer Gulf. Natural History of Spencer Gulf, Royal Society of South Australia Inc, Adelaide, 378-391.

Giri, S., & Qiu, Z. (2016). Understanding the relationship of land uses and water quality in Twenty First Century: A review. Journal of environmental management, 173, 41-48.

Han, L., & Jordan, K. (2007). Estimating and mapping chlorophyll-a concentration in Pensacola Bay, Florida using Landsat EMT+ data. International Journal of Remote Sensing, 26(23), 5245-5254. https://doi.org/https://doi.org/10.1080/01431160500219182

Haynes, D., Brodie, J., Waterhouse, J., Bainbridge, Z., Bass, D., & Hart, B. (2007). Assessment of the water quality and ecosystem health of the Great Barrier Reef (Australia): conceptual models. Environmental Management, 40, 993-1003.

Hertzfeld, M., Middleton, J. F., Andrewartha, J. R., Luick, J., & Wu, L. (2009). Chapter 1: Hydrodynamic modelling and observations of the tuna farming zone, Spencer Gulf. AquaFin CRC– Southern Bluefin Tuna aquaculture subprogram: Risk & response–Understanding the tuna farming environment. Technical report, Aquafin CRC Project, 4, 287.

Kishino, M., Takahashi, M., Okami, N., & Ichimura, S. (1985). Estimation of the spectral absorption coefficients of phytoplankton in the sea. Bulletin of marine science, 37(2), 634-642.

Koponen, S., Attila, J., Pulliainen, J., Kallio, K., Pyhälahti, T., Lindfors, A., Rasmus, K., & Hallikainen, M. (2007). A case study of airborne and satellite remote sensing of a spring bloom event in the Gulf of Finland. Continental Shelf Research, 27(2), 228-244.

Kowalczuk, P., Olszewski, J., Darecki, M., & Kaczmarek, S. (2005). Empirical relationships between coloured dissolved organic matter (CDOM) absorption and apparent optical properties in Baltic Sea waters. International Journal of Remote Sensing, 26(2), 345-370.

Kutser, T., Pierson, D., Kallio, K., Reinart, A., & Sobek, S. (2005). Mapping CDOM by satellite remote sensing. Remote Sensing of Environment, 94(4), 535-540.

Liu, H. Shah, S., Jiang, W. , "On-line outlier detection and data cleaning", Computers & Chemical Engineering, Volume 28, Issue 9, 2004.

Madrid, Y., & Zayas, Z. P. (2007). Water sampling: Traditional methods and new approaches in water sampling strategy. TrAC Trends in Analytical Chemistry, 26(4), 293-299.

Mayo, M., Gitelson, A., Yacobi, Y., & Ben-Avraham, Z. (1995). Chlorophyll distribution in Lake Kinneret determined from Landsat Thematic Mapper data. International Journal of Remote Sensing, 16(1), 175-182.

Middleton, J. F., Doubell, M., James, C. E., Luick, J., & Van Ruth, P. (2013). PIRSA Initiative II: Carrying Capacity of Spencer Gulf: Hydrodynamic and Biogeochemical Measurement Modelling and Performance Monitoring: Final Report for the Fisheries Research and Development Corporation. South Australian Research and Development Institute, SARDI Aquatic Sciences.

Middleton, J. F., Luick, J., & James, C. (2014). Carrying capacity for finfish aquaculture, Part II–Rapid assessment using hydrodynamic and semi-analytic solutions. *Aquacultural engineering*, *62*, 66-78.

Mitchell, B. G. (1990, September). Algorithms for determining the absorption coefficient for aquatic particulates using the quantitative filter technique. In Ocean optics X (Vol. 1302, pp. 137-148). SPIE.

Mobley, C.D. Estimation of the remote-sensing reflectance from above-surface measurements. Appl Optics 1999, 38, 7442-7455.

Morello, E.B., Galibert, G., Smith, D., Ridgway, K.R., Howell, B., Slawinski, D., Timms, G.P., Evans, K., Lynch, T.P., 2014. Quality control (QC) procedures for Australia's National Reference Station's sensor data-comparing semi-autonomous systems to an expert oceanographer. Methods Oceanogr. 9 (September), 17–33.

Mouw, C. B., Greb, S., Aurin, D., DiGiacomo, P. M., Lee, Z., Twardowski, M., Craig, S. E. (2015). Aquatic color radiometry remote sensing of coastal and inland waters: Challenges and recommendations for future satellite missions. Remote sensing of environment, 160, 15-30.

Nunes Vaz, R. A. N., Lennon, G. W., & Bowers, D. G. (1990). Physical behaviour of a large, negative or inverse estuary. Continental Shelf Research, 10(3), 277-304.

Pahlevan, N., Mangin, A., Balasubramanian, S.V., Smith, B., Alikas, K., Arai, K., Barbosa, C., Bélanger, S., Binding, C., Bresciani, M. and Giardino, C., 2021. ACIX-Aqua: A global assessment of atmospheric correction methods for Landsat-8 and Sentinel-2 over lakes, rivers, and coastal waters. *Remote Sensing of Environment*, *258*, p.112366.

Patricio-Valerio, L., Schroeder, T., Devlin, M. J., Qin, Y., & Smithers, S. (2022). A Machine Learning Algorithm for Himawari-8 Total Suspended Solids Retrievals in the Great Barrier Reef. Remote Sensing, 14(14), 3503.

Paxinos, R. (2007). Dynamics of phytoplankton in relation to tuna fish farms in Boston Bay and near-shore Spencer Gulf, South Australia. Flinders University, School of Biological Sciences..

Pfitzner K, Bartolo R, Carr G, Esparon A & Bollhöfer A 2011. Standards for reflectance spectral measurement of temporal vegetation plots. Supervising Scientist Report 195, Supervising Scientist, Darwin NT.

Roberts, S. D., Van Ruth, P. D., Wilkinson, C., Bastianello, S. S., & Bansemer, M. S. (2019). Marine heatwave, harmful algae blooms and an extensive fish kill event during 2013 in South Australia. Frontiers in Marine Science, 6, 610.

Ruddick, K.G., Voss, K., Boss, E., Castagna, A., Frouin, R., Gilerson, A., Hieronymi, M., Johnson, B.C., Kuusk, J., Lee, Z. and Ondrusek, M., 2019. A review of protocols for fiducial reference measurements of water-leaving radiance for validation of satellite remote-sensing data over water. Remote Sensing, 11(19), p.2198.

Seegers B, Stumpf R, Schaeffer B, Loftin K, & Werdell J. (2018). Performance metrics for the assessment of satellite data products: an ocean color case study. Optics Express, 26(6), 7404-7422.

Seuront, L., Leterme, S. C., Middleton, J., Byrne, S., James, C., Luick, J., ... & van Dongen-Vogels, V. (2010). Biophysical couplings in South Australian shelf waters under conditions of summer upwelling and winter downwelling: results from the Southern Australia Integrated Marine Observing System (SAIMOS). Proceedings of the "OceanObs, 9, 27.

Tanner, JE, M Doubell, P van Ruth, C James and J Middleton (2020). Aquaculture Environmental Monitoring Program: 2015-2019. South Australian Research and Development Institute (Aquatic

Sciences), Adelaide. SARDI Publication No. F2019/000334-1. SARDI Research Report Series No. 1053. 67pp.

Tilstone, G. H. (2004). REVAMP Protocols; Regional Validation of MERIS chlorophyll products in North Sea coastal waters., 77 pp., Working meeting on MERIS and AATSR Calibration and Geophysical Validation (MAVT 2003).

Toole, D.A.; Siegel, D.A.; Menzies, D.W.; Neumann, M.J.; Smith, R.C. Remote-sensing reflectance determinations in the coastal ocean environment: Impact of instrumental characteristics and environmental variability. Appl Optics 2000, 39, 456-469.

Vanhellemont, Q. and Ruddick, K., 2018. Atmospheric correction of metre-scale optical satellite data for inland and coastal water applications. Remote sensing of environment, 216, pp.586-597.

Wang, F., Han, L., Kung, H., & Van Arsdale, R. (2006a). Applications of Landsat-5 TM imagery assessing and mapping water quality in Reelfoot Lake, Tennessee. International Journal of Remote Sensing, 27(23), 5269-5283.

Wang, F., Han, L., Kung, H., & Van Arsdale, R. (2006b). Applications of Landsat-5 TM imagery in assessing and mapping water quality in Reelfoot Lake, Tennessee. International Journal of Remote Sensing, 27(23), 5269-5283.

Werdell, P., McKinna, L., Boss, E., Ackleson, S., Craig, S., Gregg, W., Lee, Z., Maritorena, S., Roesler, C., Rousseaux, C., Stramski, D., Sullivan, S., Twardowski, M., Tzortziou, M., & Zhang, X. (2018). An overview of appraoches and challenges for retrieving marine inherent optical properties from ocean color remote sensing. Progress in Oceanography, 160, 186-212.

Whitehead, P. G., Wilby, R. L., Battarbee, R. W., Kernan, M., & Wade, A. J. (2009). A review of the potential impacts of climate change on surface water quality. Hydrological sciences journal, 54(1), 101-123.

Wiltshire, K. H., & Tanner, J. E. (2020). Comparing maximum entropy modelling methods to inform aquaculture site selection for novel seaweed species. Ecological Modelling, 429, 109071.

Woźniak, S. (2014). Simple statistical formulas for estimating biogeochemical properties of suspended particulate matter in the southern Baltic Sea potentially useful for optical remote sensing applications. Oceanologica, 56(1), 7-39.

Woźniakc, S. (2014). Simple statistical formulas for estimating biogeochemical properties of suspended particulate matter in the southern Baltic Sea potentially useful for optical remote sensing applications. Oceanologica, 56(1), 7-39.

Zibordi, G.; Melin, F.; Voss, K.J.; Johnson, B.C.; Franz, B.A.; Kwiatkowska, E.; Huot, J.P.; Wang, M.H.; Antoine, D. System vicarious calibration for ocean color climate change applications: Requirements for in situ data. Remote Sens Environ 2015, 159, 361-369.

Appendix A:

Table A1: Project Deliverables as listed in the proposal (P3-17)

D1 – Development of project management artefacts
D2 – Sensor procurement plan
D3 – Validation test plan
D4 – Integration test results
D5 – Test and evaluation
D6 – Project close out
D7 – Lessons Learnt

USER INFORMED INDUSTRY DRIVEN RESEARCH POWERED

SMARTSAT
COOPERATIVE RESEARCH CENTRE

Australia's Premier Space Research Centre

Australian Government
Department of Industry, Science and Resources

AusIndustry
Cooperative Research Centres Program

SmartSat CRC Head Office:
Lot Fourteen, Level 2, McEwin Building
North Terrace, Adelaide, SA

info@smartsatcrc.com
smartsatcrc.com